SPRINGER BRIEFS IN BIOCHEMISTRY AND MOLECULAR BIOLOGY

Huidong Zhang

DNA Replication - Damage from Environmental Carcinogens

Springer

SpringerBriefs in Biochemistry and Molecular Biology

More information about this series at http://www.springer.com/series/10196

Huidong Zhang

DNA Replication - Damage from Environmental Carcinogens

Springer

Huidong Zhang
Institute of Toxicology, Preventive
Medical College
Third Military Medical University
Chongqing
China

ISSN 2211-9353 ISSN 2211-9361 (electronic)
SpringerBriefs in Biochemistry and Molecular Biology
ISBN 978-94-017-7211-2 ISBN 978-94-017-7212-9 (eBook)
DOI 10.1007/978-94-017-7212-9

Library of Congress Control Number: 2015940977

Springer Dordrecht Heidelberg New York London

Printed on acid-free paper

Springer Science+Business Media B.V. Dordrecht is part of Springer Science+Business Media (www.springer.com)

Preface

Environment carcinogens have been received more and more attention for human health. These carcinogens can be absorbed by cells, metabolized, and produces DNA damage, which directly affect the efficiency and fidelity of DNA replication. It has been realized that many diseases, including various cancers, are directly induced by environmental carcinogens. To understand how the carcinogens lead to diseases, firstly, we need to understand how these carcinogens lead to problems in DNA replication, because it is the first crucial factor for the integrity of genetic information and formation of mutation in life cycle. In this brief, we will discuss the DNA damage, which is formed due to the environmental carcinogens, disturbs DNA replication system through increasing the misincorporation ratio, blocking DNA replication and formation of frameshift, and destroying DNA replication by cross-linking. These researches are mainly based on DNA polymerases, and then, we will go to the level of DNA replisome, which is the complex of many proteins that perform DNA synthesis in a coordinated way. The DNA damage has obviously affected the leading- and lagging-strand DNA synthesis using the model replisome of *E. coli*, T4 and T7. Then, we further move to the level of cell. The environmental carcinogens have been identified to affect cell cycle, cell proliferation and apoptosis, and gene expression and tissue, through different and specific ways. In the last chapter, we will give the detailed protocols for studies of bypass of DNA damage by a DNA polymerase.

This brief is intended as a concise, handy overview of the main concepts that how environmental carcinogens and their corresponding DNA damage affect DNA replication and cell activities. Hopefully, this brief can provide some helpful insights for the research in biochemistry, molecular toxicology, microbiology, medicine, and cell biochemistry.

Huidong Zhang

Acknowledgments

Several qualified and enthusiastic scientists have dedicated time and made precious comments over the text and concepts presented in this brief. Binyan Liu, Juntang Yang, Changhuo Ma, and Yu Du have taken long time to assist me to prepare this brief. Mrs. Jun Zhang has carefully edited the whole text of this brief. Dr. Guengerich at Vanderbilt University has carefully read this brief and made important comments. Their hardworking, enthusiasm, and curiosity made a very important contribution to this brief.

Contents

About the Author

Dr. Huidong Zhang is a professor and assistant director at Institute of Toxicology, Preventive Medical College and Biochemistry and Molecular Biology, Third Military Medical University, PR China. He is the winner of "Thousand Youth Talents Plan" in 2013 and National Outstanding Youth Fund of PR China in 2014. Dr. Zhang got PhD of physical chemistry at Dalian Institute of Chemical Physics, Chinese Academy of Sciences. Then, he joined in F.P. Guengerich's laboratory at Vanderbilt University in 2006 and in Charles C. Richardson's laboratory at Harvard Medical School in 2009, as Postdoctoral Fellow and Senior Research Fellow. In the past seven years, Dr. Zhang has researched a single DNA polymerase bypassing DNA damage and function–structure of the T7 DNA replisome. Dr. Zhang has published 26 peer-viewed papers, containing 17 first-authored papers, such as PNAS, JBC, Cell Cycle, and JMB, including three invited papers and one cover paper. All his first-authored papers have been cited up to 511 times and two of which are more than 100 times. Additionally, Dr. Zhang is an invited reviewer for Nucleic Acids Research, Bioorganic & Medicinal Chemistry, FEBS Journal, Journal of Cellular Biochemistry, DNA Repair, Chemical Research in Toxicology, and Journal of Molecular Catalysis A: Chemistry. This group is researching in molecular toxicology, mainly focused on how environmental carcinogens affect DNA replication, genetic toxicology, and cell cancerization.

Chapter 1
DNA Replication

Abstract DNA carries genetic information that is transferred from one generation to the next. Various DNA polymerases perform accurate DNA replication. Only correct dNTP can be selected and incorporated opposite template base. DNA polymerization consists of several steps. DNA polymerases can be classified into different families, and their functional domains include thumb, palm, figure, and other assistant domains.

Keywords DNA polymerase · dNTP incorporation · Polymerization mechanism · Polymerase structure

1.1 The Mechanism of DNA Replication

DNA encodes the genetic information used in the development and functioning of all known living organisms and many viruses. Most DNA molecules consist of two strands in a double helix. Each DNA strand is composed of guanine (G), adenine (A), thymine (T), and cytosine (C), as well as a deoxyribose and a phosphate group. Hydrogen bonds between base pairs of A:T and C:G make double-stranded DNA. DNA stores biological information by its sequence of these four nucleobases. Both strands of the double-stranded structure store the same biological information.

Within cells, DNA is organized into chromosomes. During cell division, these chromosomes are duplicated, providing each cell its own complete set of chromosomes. Eukaryotic organisms (animals, fungi, plants, and protists) store most of their DNA inside the cell nucleus and some of their DNA in organelles, such as mitochondria or chloroplasts. Prokaryotes (archaea and bacteria) store their DNA only in the cytoplasm. Within the chromosomes, chromatin proteins compact and organize DNA. These compact structures guide the protein–DNA interactions, regulating DNA replication.

One original DNA molecule can be replicated into two identical replicas. This biological process is the basis for biological inheritance. Each strand of the original DNA molecule serves as template for the production of the complementary strand, a

H. Zhang, *DNA Replication - Damage from Environmental Carcinogens*,
SpringerBriefs in Biochemistry and Molecular Biology 17,
DOI 10.1007/978-94-017-7212-9_1

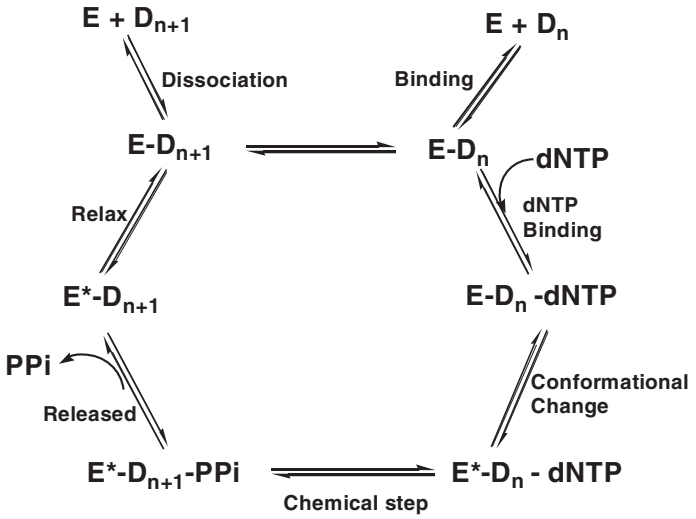

Fig. 1.1 The mechanism of single dNTP incorporation. *E* DNA polymerase, *Dn* DNA substrate, *E** conformationally changed DNA polymerase, D_{n+1} DNA substrate extended by one base (product), *PPi* pyrophosphate. The "chemical step" is also termed phosphodiester bond formation or nucleotidyl transfer

process referred to as semiconservative replication. Each strand of DNA is replicated from 5′ to 3′; therefore, both strands of DNA are replicated in opposite directions.

DNA replication is performed by DNA polymerases. For most of the DNA replication, only the correct dNTP is selected to make standard W-C base pairing with template base and is rapidly incorporated at the 3′ end of the primer. The unpaired dNTPs are repulsed outside the active site or incorporated very inefficiently. Most DNA polymerases catalyze single dNTP incorporation according to a general mechanism (Fig. 1.1). DNA polymerase binds DNA to form a binary complex. This binary complex selectively binds correct dNTP based on Watson–Crick base pairing to form a polymerase–DNA–dNTP ternary complex, followed by inducing a conformational change to facilitate the formation of the phosphodiester bond. After the chemical reaction (nucleotidyl transfer), pyrophosphate is released and the binary complex is relaxed to initiate a new cycle. Some DNA polymerases, such as T7 DNA polymerase, have revealed a nucleotide-induced conformational change. Efficient polymerization is dependent on the selection of correct dNTP, conformational change, and phosphodiester bond formation. Therefore, these three steps are considered as three checkpoints to control the fidelity of a DNA polymerase. Single-molecule FRET studies have shown that only the closed conformation is observed upon correct dNTP binding, which stabilizes the polymerase–DNA–dNTP ternary complex, whereas incorrect dNTPs destabilize the complex.

1.2 Classification and Structure of DNA Polymerases

DNA replication is performed by various DNA polymerases. At least seven families of DNA polymerases have been classified based on their sequence and structural similarities: A, B, C, D, X, Y, and reverse transcriptase. Each family has specific functions in DNA polymerization. Generally, Y-family polymerases carry out translesion DNA synthesis, and A-family DNA polymerases perform fast and accurate DNA replication.

DNA polymerases of humans, yeast, *Sulfolobus solfataricus*, *Escherichia coli*, and bacteriophage T7 have been extensively studied. Humans possess at least 19 enzymes: pols α, δ, ε, and ζ belong to B-family; mitochondrial pol γ and pols ν and θ belong to A-family; pols β, λ, and μ belong to X-family; pols η, ι, and κ and REV1 belong to Y-family; and other enzymes are pols $\sigma 1$, $\sigma 2$, φ, terminal deoxynucleotidyl transferase, and telomerase. DNA polymerases of yeast are similar but not identical to those of human. *E. coli* and some other prokaryotes have five DNA polymerases. A-family pols I and II assist replication (or repair). C-family Pol III is the major replicative polymerase for fast and accurate DNA replication. Polymerases IV and V are Y-family members for bypass of DNA damage and facilitation of adaptive mutation. The *S. solfataricus* has three B-family DNA polymerases (Dpo1, Dpo2, and Dpo3) and one Y-family DNA polymerase (Dpo4) for translesion DNA synthesis. Bacteriophage T7 has only one A-family DNA polymerase, gene 5 protein (gp5), with high fidelity in DNA replication.

DNA polymerases consist of thumb, palm, and finger domains, holding DNA in a right-hand mode. A-family T7 DNA polymerase has a tight active site, into which only standard Watson–Crick base pairs can fit. Differently, Y-family DNA polymerases have more open and flexible active sites and can accommodate bulky DNA damage. Additionally, little finger (or PAD) domain is also present in Y-family DNA polymerases. Subtle variations in the little finger domain are important for bypass of DNA damage for different Y-family members. *S. solfataricus* Y-family DNA polymerase Dpo4 is comprised of the palm domain (containing the catalytic residues), the finger domain (playing a role in nucleotide selectivity), the thumb domain (making important contacts with DNA substrate), and the little finger domain (believed to play an important role in lesion bypass and polymerase processivity). Pol κ also has an additional region, referred as N-clasp, which is comprised of two α-helical elements that are placed directly above the DNA substrate to encircle DNA.

Further Reading

Copeland WC (2008) Inherited mitochondrial diseases of DNA replication. Ann Rev Medicine 59:131–146.

Kelman Z, Donnell MO (1995) DNA polymerase III holoenzyme: structure and function of a chromosomal replicating machine. Annu Rev Biochem 64:171–200.

McHenry CS (1988) DNA polymerase III holoenzyme of Escherichia coli. Annu Rev Biochem 57: 519–550.

Goodman MF (2002) Error-prone repair DNA polymerases in prokaryotes and eukaryotes. Annu Rev Biochem 71:17–50.

Loeb LA, Monnat RJ (2008) DNA polymerases and human disease. Nat Rev Gen 9: 594–604.

Doublie S, Tabor S, Long AM, Richardson CC, Ellenberger T (1998) Crystal structure of a bacteriophage T7 DNA replication complex at 2.2 angstrom resolution. Nature 391:251–258.

Wang J, Sattar AA, Wang C, Karam J, Konigsberg W, Steitz T (1997) Crystal structure of a pol α family replication DNA polymerase from bacteriophage RB69. Cell 89:1087–1099.

Ling H, Boudsocq F, Woodgate R, Yang W (2001) Crystal structure of a Y-family DNA polymerase in action: a mechanism for error-prone and lesion-bypass replication. Cell 107:91–102.

Jarosz DF, Beuning PJ, Cohen SE, Walker GC (2007) Y-family DNA polymerases in Escherichia coli. Trends Microbiol 15:70–77.

Lone S, Townson SA, Uljon SN, Johnson RE, Brahma A, Nair DT, Prakash S, Prakash L, Aggarwal AK (2007) Human DNA polymerase kapa encircles DNA: implications for mismatch extension and lesion bypass. Mol Cell 25:601–614.

Zhang H, Guengerich FP (2010) Effect of N-2-Guanyl Modifications on Early Steps in Catalysis of Polymerization by Sulfolobus solfataricus P2 DNA Polymerase Dpo4 T239 W. J Mol Biol 395:1007–1018.

Brenlla A, Markiewicz RP, Rueda D, Romano LJ (2013) Nucleotide selection by the Y-family DNA polymerase Dpo4 involves template translocation and misalignment. Nucl Acids Res 42: 2555–2563.

Eoff RL, Irimia A, Angel KC, Egli M, Guengerich P (2007) Hydrogen bonding of 7,8-dihydro-8-oxodeoxyguanosine with a charged residue in the little finger domain determines miscoding events in Sulfolobus solfataricus DNA polymerase Dpo4. J Biol Chem 282: 19831–19843.

Chapter 2
Disturbances of the DNA Replication System

Abstract DNA damage leads to mutation, and bulky DNA damage blocks DNA replication. DNA damage also increases the misincorporation ratio by reducing the correct incorporation efficiency, by increasing the misincorporation efficiency, or by both. DNA damage can also produce frameshifts. DNA–DNA cross-linking can destroy DNA replication.

Keywords Misincorporation ratio · Incorporation efficiency · Blockage of DNA replication · Frameshift · Cross-linking

The molecular mechanisms of mutation caused by DNA damage are still poorly analyzed. Some recent reviews have described various DNA damage, individual DNA polymerase, and information about how these polymerases bypass DNA damage. Herein, based on our own work and recent progress in this area, we analyze these data and proposed four major pathways by which DNA damage leads to mutation: blocking DNA replication, increasing misincorporation ratio, producing frameshifts, and destroying DNA replication by cross-linking.

2.1 DNA Damage Blocks DNA Replication

DNA damage blocks DNA replication. The blockage means that the incoming dNTP cannot form the phosphodiester bond with the 3′-OH at the primer end. At least three reasons can explain these possibilities. Firstly, the incoming dNTP is repulsed outside of the active site and is far away from 3′-OH at the primer end, such as in the case of N^2,N^2-diMeG. Secondly, the incoming dNTP is accommodated at the active site but paired with the template base via nonstandard W-C pairing modes, such as in the case of $N^{2,3}$-εG. Thirdly, the DNA adduct is too bulky to be accommodated and/or disordered in the active site, e.g., PAH-DNA adducts, CPD, DNA-protein cross-link adducts, and AAF. All of these configurations lead to the blockage of DNA replication.

H. Zhang, *DNA Replication - Damage from Environmental Carcinogens*,
SpringerBriefs in Biochemistry and Molecular Biology 17,
DOI 10.1007/978-94-017-7212-9_2

Repulsion of dNTP outside the active site: T7 DNA polymerase, HIV reverse transcriptase, pol κ, pol ι, pol η, and Dpo4 were strongly blocked by N^2,N^2-dialkylG. The efficiency of dCTP incorporation against N^2,N^2-dialkylG was decreased 160,000-fold compared with unmodified G for Dpo4, blocking DNA replication. No obvious fast conformational change was observed, indicating that N^2,N^2-Me_2G strongly perturbs the conformational change. Nearly no burst was observed for the incorporation of dCTP opposite N^2,N^2-Me_2G, indicating less than 5 % active polymerase–DNA–dCTP ternary complex. DNA replication is strongly blocked upon encountering this lesion. The crystal structures showed that the 3′-terminal dideoxycytosine of the primer that should pair with the template N^2,N^2-Me_2G is repulsed outside of the active site and folded back into the minor groove, as a catalytically incompetent complex, explaining the blockage of dNTP incorporation.

Nonstandard W-C paring mode: Lipid peroxidation or oxidation products of vinyl monomers can produce exocyclic adduct N^2,3-εG, which blocks human DNA pol ι and REV1, yielding only 1-base incorporation opposite this lesion. Structurally, pol ι can accommodate an N^2,3-εG:dCTP base pair rather well at the active site without significant conformational changes of protein or nucleic acid, but the phosphate group of the incoming dCTP and primer terminus 3′-OH is misaligned. Two hydrogen bonds were observed in the N^2,3-εG:dCTP base pair, whereas only one appears in the N^2,3-εG:dTTP pair.

Bulkier adducts disordering active site: The reactive 7,8-diol-9,10-epoxides of benzo[a]pyrene form N^2-B[a]P guanine and N^6-B[a]P adenine adducts, which strongly block dNTP incorporation. dATP is preferentially incorporated by T7 DNA polymerase, but the catalytic efficiency is decreased by at least four orders of magnitude. No fast burst phases were observed for dNTP incorporation opposite all of these lesions, indicating that the rate-limiting step is at or before phosphodiester bond formation. Dpo4 gave the same results as T7 DNA polymerase in bypassing N^6-B[a]P A. The incorporation is blocked and dATP was preferably inserted. Crystal structure of Dpo4 containing this lesion shows that polymerization of incoming dNTP with the 3′-OH at the primer end is inhibited because both of which are separated beyond for a chemical reaction. Mouse pol κ can bypass N^2-B[a]P G efficiently and accurately, but a mutant with the reduced gap size was strongly blocked by this lesion, suggesting that the presence of this gap is essential for the DNA adduct bypass. Structurally, the gap physically accommodates the bulky aromatic adduct and keeps the active site ordered, explaining crucial functions of the gap in pol κ in maintenance of the active site for translesion DNA synthesis.

Human pol κ can insert dATP opposite the 5′-T of a cis-syn T-T dimer but cannot insert nucleotides opposite the 3′-T of the dimer, leading to the blockage of DNA replication. Structurally, the active site of pol κ can only accommodate the incoming dATP with the 5′-T of the T-T dimmer, leaving the 3′-T misaligned at active site and blocking DNA replication. Single-molecule fluorescence resonance energy transfer (smFRET) and protein-induced fluorescence enhancement (smPIFE) experiments show that *Escherichia coli* DNA polymerase I (Klenow fragment) binds to AAF-dG in an intermediate orientation, which is very unstable, and then rapidly transfers DNA from the active site to a more stable exonuclease site, thus blocking DNA replication.

2.2 DNA Damage Increases Misincorporation Ratio

Misincorporation ratio is dependent on the relative efficiency of correct dNTP incorporation relative to misincorporation. Correct incorporation is much faster than incorrect ones for most DNA polymerases. In the presence of DNA adducts, the incorporation efficiency may decrease and/or the incorrect incorporation efficiency may increase, increasing misincorporation ratio.

Decreasing correct incorporation efficiency: Some DNA adducts reduce only correct incorporation efficiency but do not affect the misincorporation, for example, N^2-alkylG and O^6-alkylG adducts.

The bypass of N^2-alkylG adducts has been studied by *Sulfolobus solfataricus* Dpo4. Dpo4 preferentially incorporates dCTP opposite to these adducts, but incorporation efficiencies (k_{cat}/K_m) are decreased 3- to 125-fold compared with the unmodified G. The misincorporation efficiencies remain almost unchanged, thus reducing incorporation fidelities by 100-fold. Some bulkier N^2-alkylG also strongly perturbs the fast conformation change. X-ray crystal structures show that the incoming dCTP is severely buckled and locates outside the active site if N^2-NaphG residue is in the *trans*-form, indicating a nonproductive complex; dCTP can also pair with the *cis*-form of the N^2-NaphG residue via a Hoogsteen mode to continue DNA polymerization. For N^2,N^2-Me_2G, the dCTP incorporation efficiency (k_{cat}/K_m) was drastically decreased by 16,000-fold compared with G, but the misincorporation frequencies are almost unchanged, increasing the misincorporation ratios up to 0.36–2.3. N^2,N^2-Me_2G leads to a random misincorporation and completely destroying the incorporation fidelity.

O^6-MeG and O^6-BzG were also studied by Dpo4. Compared with unmodified G, incorporation of dCTP opposite O^6-MeG is inhibited by three orders of magnitude, but the misincorporation efficiencies are unchanged, thus reducing the incorporation fidelity by three orders of magnitude compared with unmodified G. Finally, about 70 % of dCTP, 20 % of dTTP, and 10 % of dATP were incorporated opposite O^6-MeG. Bypass of O^6-BzG is similar to O^6-MeG except for a greater decrease in incorporation efficiency. The dCTP incorporation efficiency is strongly inhibited by 5000-fold for O^6-BzG compared with G while the misincorporation efficiencies are reduced only 10-fold, finally decreasing the incorporation fidelity about three orders compared with unmodified G. Structurally, O^6-MeG:C or O^6-BzG:C formed a wobble base pair with two hydrogen bonds between O^6-alkylG lesions and dCTP, shifting the base-pairing orientation from the standard W-C mode to the wobble mode, thus decreasing the correct incorporation efficiency.

Increasing incorrect incorporation efficiency: Some DNA adducts only partially affect the correct incorporation efficiency but drastically increase the misincorporation efficiency, thus reducing incorporation fidelity, for example, 8-oxoG.

The efficiency of incorporation of dCTP opposite 8-oxoG is decreased 80-fold compared with unmodified G for human DNA polymerase κ (hpol κ), but dATP misincorporation efficiency is increased 100-fold compared with unmodified G. Therefore, the incorporation fidelity was decreased 8000-fold for 8-oxoG compared with unmodified G, leading to a conversion from G:C pairing to T:A

pairing. In the pre-steady-state kinetic analysis, the efficiency ($k_{pol}/K_{d,dCTP}$) for the insertion of dCTP opposite 8-oxoG was decreased 65-fold compared with G, but dATP incorporation showed a fast burst, different from the absence of burst for the incorporation of dATP opposite G. The catalytic efficiency ($k_{pol}/K_{d,dCTP}$) for insertion of dATP opposite 8-oxoG is increased up to 0.63 s^{-1} μM^{-1}, 20-fold higher than that for incorporation of dCTP opposite 8-oxoG. From structures, the N-terminal extension of hpol κ stabilizes its little finger domain, which surrounds the Hoogsteen base pair of 8-oxoG and incoming dATP, explaining the increase in efficiency for the incorporation of dATP opposite 8-oxoG.

For Dpo4, the insertion of dCTP opposite G or 8-oxoG has similar catalytic efficiency, whereas the efficiency for incorporation of dATP opposite 8-oxoG was increased 250-fold compared with G, thus decreasing fidelity 200-fold opposite 8-oxoG relative to unmodified G. Crystal structures show that the Arg-332 residue in the little finger domain of Dpo4 can form a hydrogen bond with the oxygen atom at the C8 position of 8-oxoG and stabilizes the Watson–Crick base pair of incoming dCTP and 8-oxoG. Notably, no stabilization function is observed for W-C pairing of 8-oxoG and dCTP at the active site of hpol κ. The Hoogsteen pairing of 8-oxoG:dATP is favorable relative to 8-oxoG:dCTP pair in hpol κ, leading to structurally different bypass of 8-oxoG by Dpo4 and hpol κ.

2.3 DNA Damage Forms Frameshift During DNA Replication

DNA damage leads to frameshifts by adding or subtracting nucleotides in the newly synthesized DNA strand, disturbing DNA sequence, genetic information, RNA transcription, and protein expression. -1 frameshift means one nucleotide is missing after DNA replication. Four different mechanisms have been proposed to explain how -1 deletion frameshifts are produced (Fig. 2.1).

Streisinger template-slippage mechanism: -1 frameshift produced in the replication of repetitive DNA sequences can be explained by Streisinger template-slippage mechanism. The primer misaligns on a repetitive template DNA strand, forming an unpaired template base in the newly synthesized DNA, that is, one base shorter than the original template. Y-family DNA polymerase Dbh generates -1 frameshift in repetitive sequences with error frequencies up to 50 %. In the crystal structure of Dbh, a cleft between the polymerase domain and the C-terminal domain provides ample space to accommodate extrahelical template bases. Tyr-249 and Arg-333 in the C-terminal domain stabilize the extrahelical base at the -3 position of template, and residues in the flexible loop of Dbh interact with the bulged base at the -2 position of template. Therefore, Dbh does not appear to strictly regulate the entry of template bases into the active site, allowing template misalignment to occur more readily.

Misincorporation–misalignment mechanism: dNTP is firstly misincorporated and then the template misaligns so that dNTP can pair with the next template base

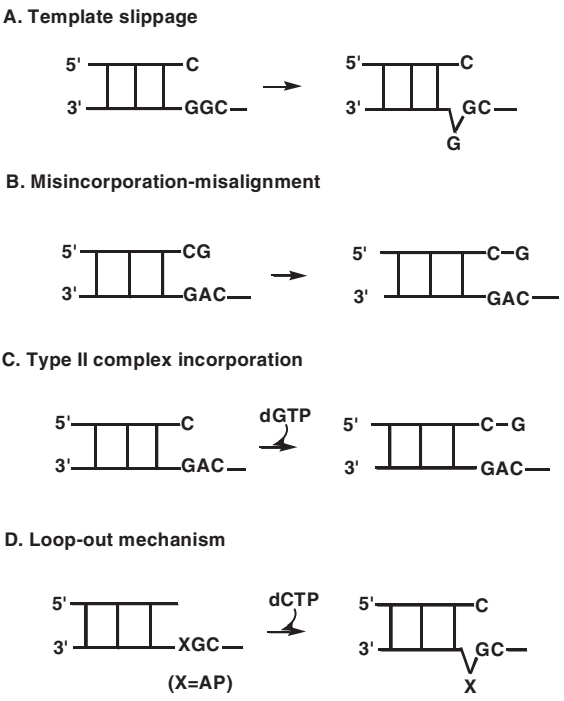

Fig. 2.1 Four mechanisms are proposed for the formation of -1 deletion frameshifts

correctly. DNA polymerase I (Klenow fragment) of bacteriophage M13mp2 catalyzes DNA replication on M13 dsDNA containing a 361-nucleotide ssDNA gap using an imbalanced dNTP pool. -1 frameshifts are preferentially formed when the template sequence has a 5′-neighbor nucleotide that is complementary to the dNTP provided in excess. When a dNTP complementary to the 5′-next nucleotide in the template is first misincorporated opposite a template nucleotide, this misincorporated nucleotide then misaligns and correctly pairs with the next complementary template nucleotide, forming a correct terminal base pair and -1 frameshift. If the mispaired nucleotide at the end of primer is complementary to the 5′-next template nucleotide, the in vivo frequency of -1 frameshift deletion was 58-fold higher than if the nucleotide at the primer end was non-complementary to the 5′-template nucleotide, reflecting the misincorporation–misalignment mechanism.

dNTP-stabilized misalignment mechanism: This mechanism is also called as Type II complex mechanism. Dpo4 produces -1 frameshifts. 0–2 % frameshifts are produced with thymine or cytosine at the incorporation position, 9–12 % with adenine or guanine, and 25–50 % with larger planar cyclic DNA adducts, e.g., 1,N^2-ε-G, which has the strongest stacking interaction with the incoming dNTP. In crystal structures, purines and larger planar DNA adduct at the incorporation position can stack with the incoming dNTP that has paired with the next template base, forming a Type II complex. The conformational change of Dpo4 upon forming the Type II complex is very fast, followed by a slow step for the formation of phosphodiester bond.

Loop-out mechanism: A loop-out mechanism is also proposed to explain the formation of -1 frameshift. In the bypass of an abasic site by *S. solfataricus* Dpo4, the abasic site in the template cannot base stack with an incoming dNTP and then loops out from the duplex. The incoming dNTP subsequently pairs with the 5′ next template base. In crystal structures, the abasic lesion that loops out can be accommodated in the cavity between the fingers and little finger domains of Dpo4.

2.4 DNA–DNA Cross-Linking Destroys DNA Replication

1,3-butadiene (BD), which belongs to bis-electrophilic agents, can produce DNA–DNA or DNA–protein cross-links. BD can be oxidized to 1,2,3,4-diepoxybutane (DEB) (Fig. 2.2). Alkylation of adenine or guanine base by DEB produces 2-hydroxy-3,4-epoxybut-1-yl (HEB) DNA lesion, which contains an inherently reactive oxirane group that can further alkylate neighboring nucleotide bases within the DNA duplex to form DNA–DNA cross-links. The 3,4-epoxy ring can also produce DNA–protein cross-links by nucleophilic attack by amino acid groups in side chains of neighboring proteins. DEB reacting with a protein such as O^6-alkylG DNA alkyltransferase or the tripeptide glutathione is also documented and probably more likely. Acrolein and other α,β-unsaturated aldehydes from cigarette smoke and automobile exhaust can also cross-link (inter-strand) DNA in a similar pathway.

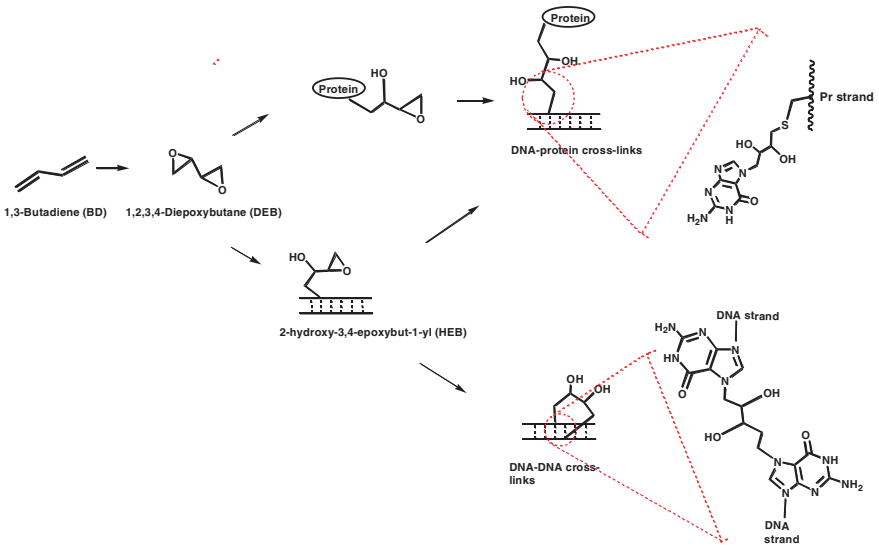

Fig. 2.2 Formation of DNA–DNA or DNA–protein cross-links involving an oxidation product of 1,3-butadiene (BD) (*Pr* protein)

The cross-linking adducts block A-family DNA polymerases. Translesion DNA polymerases, such as *E. coli* pol IV and pol V, are also incapable of bypassing the cross-links. Crystal structures of these complexes have not been reported yet, but the general opinion is that these adducts are too bulky to be accommodated by the active sites of DNA polymerases. However, hpol κ can efficiently bypass DNA-peptide cross-links if the peptide is N-substituted and linked to the N2 position of G, which can be considered an N^2-alkylG adduct. The crystal structure of the complex containing N^2-alkylG shows that pol κ completely encircles the DNA duplex using its unique N-terminal extension. This kind of structure may be flexible enough in the hinge domain to allow pol κ to pass through these kinds of cross-linked bulky lesions.

Further Reading

Irimia A, Eoff RL, Guengerich FP, Egli M (2009) Structural and functional elucidation of the mechanism promoting error-prone synthesis by human DNA polymerase kappa opposite the 7,8-Dihydro-8-oxo-2 '-deoxyguanosine adduct. J Biol Chem 284:22467–22480.

Zang H, Irimia A, Choi JY, Angel KC, Loukachevitch LV, Egli M, Guengerich FP (2006) Efficient and high fidelity incorporation of dCTP opposite 7,8-dihydro-8-oxodeoxyguanosine by Sulfolobus solfataricus DNA polymerase Dpo4. J Biol Chem 281:2358–2372.

Eoff RL, Irimia A, Angel KC, Egli M, Guengerich P (2007) Hydrogen bonding of 7,8-dihydro-8-oxodeoxyguanosine with a charged residue in the little finger domain determines miscoding events in Sulfolobus solfataricus DNA polymerase Dpo4. J Biol Chem 282:19831–19843.

Zhao L, Pence MG, Christov PP, Wawrzak Z, Choi JY, Rizzo CJ, Egli M, Guengerich FP (2012) Basis of Miscoding of the DNA Adduct N^2,3-Ethenoguanine by Human Y-family DNA Polymerases. J Biol Chem 287:35516–35526.

Zhang H, Eoff RL, Kozekov ID, Rizzo CJ, Egli M, Guengerich FP (2009) Structure-Function Relationships in Miscoding by Sulfolobus solfataricus DNA Polymerase Dpo4 guanine N2,N2-dimethyl substiton produces inactive and miscoding polymerase complexes. J Biol Chem 284:17687–17699.

Zang H, Chowdhury G, Angel KC, Harris TM, Guengerich FP (2006) Translesion synthesis across polycyclic aromatic hydrocarbon diol epoxide adducts of deoxyadenosine by *Sulfolobus solfataricus* DNA polymerase Dpo4. Chem Res Toxicol 19:859–867.

Vasquez-Del Carpio R, Silverstein TD, Lone S, Johnson RE, Prakash L, Prakash S, Aggarwal AK (2011) Role of Human DNA Polymerase kappa in Extension Opposite from a cis-syn Thymine Dimer. J Mol Biol 408:252–261.

Minko IG, Yamanaka K, Kozekov ID, Kozekova A, Indiani C, O'Donnell ME, Jiang Q, Goodman MF, Rizzo CJ, Lloyd RS (2008) Replication bypass of the acrolein-mediated deoxyguanine DNA-peptide cross-links by DNA polymerases of the DinB family. Chem Res Toxicol 21:1983–1990.

Vrtis KB, Markiewicz RP, Romano LJ, Rueda D (2013) Carcinogenic adducts induce distinct DNA polymerase binding orientations. Nucl Acids Res 41:7843–7853.

Choi JY, Guengerich FP (2006) Kinetic evidence for efficient and error-prone bypass across bulky N^2-guanine DNA adducts by human DNA polymerase *i*. J Biol Chem 281:12315–12324.

Choi JY, Angel KC, Guengerich FP (2006) Translesion synthesis across bulky N^2-alkylguanine DNA adducts by human DNA. J Biol Chem 2006:21062–21072.

Choi JY, Guengerich FP (2005) Adduct size limits efficient and error-free bypass across bulky N^2-guanine DNA lesions by human DNA polymerase η. J Mol Biol 352:72–90.

Choi YJ, Guengerich FP (2004) Analysis of the effect of bulk at N^2-alkylguanine DNA adducts on catalytic efficiency and fidelity of the processive DNA polymerase T7 exonuclease$^-$ and HIV-1 reverse transcriptase. J Biol Chem 279:19217–19229.

Zhang H, Guengerich FP (2010) Effect of N-2-Guanyl Modifications on Early Steps in Catalysis of Polymerization by Sulfolobus solfataricus P2 DNA Polymerase Dpo4 T239 W. J Mol Biol 395:1007–1018.

Zang H, Harris TM, Guengerich FP (2005) Kinetics of nucleotide incorporation opposite polycyclic aromatic hydrocarbon - DNA adducts by processive bacteriophage T7 DNA polymerase. Chem Res Toxicol 18:389–400.

Ling H, Sayer JM, Plosky BS, Yagi H, Boudsocq F, Woodgate R, Jerina DM, Yang W (2004) Crystal structure of a benzo[*a*]pyrene diol epoxide adduct in a ternary complex with a DNA polymerase. Proc Natl Acad Sci U S A 101:2265–2269.

Kirouac KN, Basu AK, Ling H (2013) Structural Mechanism of Replication Stalling on a Bulky Amino-Polycyclic Aromatic Hydrocarbon DNA Adduct by a Y Family DNA Polymerase. J Mol Biol 425:4167–4176.

Liu Y, Yang Y, Tang TS, Zhang H, Wang Z, Friedberg E, Yang W, Guo C (2014) Variants of mouse DNA polymerase reveal a mechanism of efficient and accurate translesion synthesis past a benzo[a]pyrene dG adduct. Proc Natl Acad Sci U S A 111:1789–1794.

Ling H, Boudsocq F, Woodgate R, Yang W (2001) Crystal structure of a Y-family DNA polymerase in action: a mechanism for error-prone and lesion-bypass replication. Cell 107:91–102.

Zhang H, Beckman JW, Guengerich FP (2009) Frameshift Deletion by Sulfolobus solfataricus P2 DNA Polymerase Dpo4 T239 W Is Selective for Purines and Involves Normal Conformational Change Followed by Slow Phosphodiester Bond Formation. J Biol Chem 284:35144–35153.

Zang H, Goodenough AK, Choi JY, Irimia A, Loukachevitch LV, Kozekov ID, Angel KC, Rizzo CJ, Egli M, Guengerich FP (2005) DNA adduct bypass polymerization by Sulfolobus solfataricus DNA polymerase Dpo4 - Analysis and crystal structures of multiple base pair substitution and frameshift products with the adduct 1,N-2-ethenoguanine. J Biol Chem 280:29750–29764.

Streisinger G, Okada Y, Emrich J, Newton J, Tsugita A, Terzaghi E, Inouye M (1966) Cold Spring Harbor Symposia on Quantitative Biology. Cold Spring Harbor Laboratory Press 31:77–84.

Wilson RC, Pata JD (2008) Structural insights into the generation of single-base deletions by the Y family DNA polymerase dbh. Mol Cell 29:767–779.

Kunkel TA, Alexander PS (1986) The base substitution fidelity of eucaryotic DNA polymerases: mispairing frequencies, site preferences, insertion preferences, and base substitution by dislocation. J Bio Chem 261:160–166.

Bebenek K, Kunkel TA (1990) Frameshift errors initiated by nucleotide misincorporation. Proc Natl Acad Sci U S A 87:4946–4950.

Kunkel TA, Soni A (1988) Mutagenesis by transient misalignmen. J Biol Chem 263:14784–14789.

Fiala KA, Hypes CD, Suo Z (2007) Mechanism of abasic lesion bypass catalyzed by a Y-family DNA polymerase. J Biol Chem 282:8188–8198.

Ling H, Boudsocq F, Woodgate R, Yang W (2004) Snapshots of replication through an abasic lesion; structural basis for base substitutions and frameshifts. Mol Cell 13:751–762.

Lone S, Townson SA, Uljon SN, Johnson RE, Brahma A, Nair DT, Prakash S, Prakash L, Aggarwal AK (2007) Human DNA polymerase kapa encircles DNA: implications for mismatch extension and lesion bypass. Mol Cell 25:601–614.

Brenlla A, Markiewicz RP, Rueda D, Romano LJ (2013) Nucleotide selection by the Y-family DNA polymerase Dpo4 involves template translocation and misalignment. Nucleic Acids Res 42:2555–2563.

Zhang H, Eoff RL, Kozekov ID, Rizzo CJ, Egli M, Guengerich FP (2009) Versatility of Y-family Sulfolobus solfataricus DNA Polymerase Dpo4 in Translesion Synthesis Past Bulky N-2-Alkylguanine Adducts. J Biol Chem 284:3563–3576.

Zhang H, Bren U, Kozekov ID, Rizzo CJ, Stec DF, Guengerich FP (2009) Steric and Electrostatic Effects at the C2 Atom Substituent Influence Replication and Miscoding of the DNA Deamination Product Deoxyxanthosine and Analogs by DNA Polymerases. J Mol Biol 392:251–269.

Eoff RL, Irimia A, Egli M, Guengerich FP (2007) *Sulfolobus solfataricus* DNA polymerase Dpo4 is partially inhibited by "Wobble" pairing between O^6-methylguanine and cytosine but accurate bypass is preferred. J Biol Chem 282:1456–1467.

Eoff RL, Angel KC, Egli M, Guengerich FP (2007) Molecular basis of selectivity of nucleoside triphosphate incorporation opposite O^6-benzylguanine by *Sulfolobus solfataricus* DNA polymerase: steady-state and pre-steady-state kinetics and x-ray crystallography of correct and incorrect pairing. J Biol Chem 282:13573–13584.

Chapter 3
Fate of DNA Replisome upon Encountering DNA Damage

Abstract The real DNA replication in cell is performed by DNA replisome. Herein, we will discuss the *Escherichia coli*, T4 and T7 DNA replisome. When DNA replisome encounters DNA damage, the replisome will have different fates. Some DNA replisome bypass DNA damage with the aid of protein interactions or other assistant proteins in the replisome. Other replisome will dissociate according to some specific pathways.

Keywords DNA replisome · DNA damage · T7 DNA replisome · T4 DNA replisome · *E. coli* replisome

3.1 The DNA Replisome of *E. coli*, T7 and T4

DNA replication in vivo is performed by the DNA replisome. DNA replisomes mediate assembly of proteins at the replication fork, unwinding of DNA, template-directed polymerization of nucleotides, and synthesis of RNA primers. A major role of the replisome is to coordinate DNA polymerization mediated by its protein constituents, so that leading- and lagging-strand DNA synthesis proceed at the same rates. The replisome is a dynamic structure, involving the release and recruitment of proteins as the replisome proceeds. The complexity of the DNA replisome results from protein interactions and various functions of accessory proteins within the complex. The DNA replisomes of *Escherichia coli* and bacteriophages T7 and T4 have been constructed in vitro.

The T7 DNA replisome contains gene 5 DNA polymerase (gp5), gene 4 helicase–primase (gp4), the *E. coli* processivity factor thioredoxin (trx), and gene 2.5 ssDNA binding protein (gp2.5). Gp5 and trx form a high-affinity complex (gp5/trx) to increase the processivity of nucleotide polymerization. The helicase at the C-terminal domain of gp4 assembles as a hexamer and unwinds dsDNA to yield two ssDNA templates for leading- and lagging-strand DNA synthesis. Gp2.5 coats ssDNA to remove secondary structures and also physically interacts with gp5/trx, interactions essential for coordination of leading- and lagging-strand DNA synthesis.

H. Zhang, *DNA Replication - Damage from Environmental Carcinogens*,
SpringerBriefs in Biochemistry and Molecular Biology 17,
DOI 10.1007/978-94-017-7212-9_3

The T4 DNA replisome consists of DNA polymerase, helicase, ssDNA binding protein, a trimetric clamp processivity factor, a pentameric clamp-loader complex, and six monomers of the primase. The DNA polymerase has polymerase and exonuclease activities. A clamp-loading complex contains four molecules of the gene 44 protein and one molecule of the gene 62 protein. T4 DNA polymerase is monomeric, but it forms a dimer (via a disulfide bond) when bound to primer–template.

The *E. coli* DNA replisome comprises DNA polymerase III holoenzyme, DnaB helicase, DnaG primase, ssDNA binding protein, and multiple accessory proteins. The Pol III holoenzyme consists of a three-subunit catalytic core (α-polymerase, ε-exonuclease, and θ), a homodimeric β processivity clamp, and a $\delta\delta'\tau_2\gamma\chi\varphi$-clamp-loader complex. The β clamp consists of ring-shaped dimeric proteins that encircle DNA and bind to the Pol III core, thereby giving the DNA polymerase high processivity. The clamp-loader complex opens and loads the β clamp onto a primed site. Each τ subunit binds to the DnaB helicase and one Pol III core polymerase, coupling the helicase and the polymerase.

The T7 DNA replisome contains only four proteins, but the replisomes of *E. coli* and bacteriophage T4 contain thirteen and eight proteins, respectively, most of which are accessory proteins. These accessory proteins have roles in protein interaction in the bacteriophage T7 system. In mammals, including humans, the DNA replisome is too complicated to be constructed at this point, and only simple replication complexes have been reported in vitro.

DNA replisomes have shown different patterns of DNA synthesis from systems using a single DNA polymerase. The differences mainly result from two major reasons: protein–protein interactions and accessory proteins in DNA replisome that facilitate DNA polymerase to bypass damage as described below.

3.2 The *E. coli* DNA Replisome Bypassing DNA Damage

DNA replication machinery constantly encounters DNA lesions under normal growth conditions. Cox et al. have estimated that 10–50 % of all replication forks may be subjected to collapse in one generation of a single cell. Translesion DNA synthesis by single DNA polymerases may not reflect the accurate situation in vivo. Therefore, translesion DNA synthesis using DNA replisomes should be the object of more studies.

Addition of ddTTP can selectively block leading-strand DNA synthesis. The fate of *E. coli* DNA replisome was studied after the leading-strand DNA synthesis is blocked. The leading-strand polymerase remains stably bound to the helicase at the replication fork. The helicase continues to unwind DNA for ~1 kb ahead of the blocked leading-strand polymerase. The lagging-strand polymerase is connected to the stalled leading-strand polymerase and remains active in converting the lagging ssDNA to duplex DNA. When the lagging-strand DNA polymerase is blocked by a DNA lesion on the lagging strand, the leading- and lagging-stand DNA polymerases remain physically coupled, but functionally uncoupled. The

leading-strand polymerase continues unabatedly, allowing the replication fork to continue. This action causes a large loop of ssDNA to accumulate on the lagging-strand template. This loop grows until the supply of ssDNA binding protein is depleted. At that point, the naked ssDNA triggers the release of the stalled lagging-strand polymerase from the blocked site and resumes the synthesis of a new Okazaki fragment on a newly primed site.

After encountering a CPD DNA lesion at leading-strand template, the *E. coli* DNA replisome is only transiently blocked, which is then reinitiated downstream of the damage, dependent on the assistance of primase DnaG in the DNA replisome but not on any other known replication-restart proteins. Therefore, the *E. coli* DNA replisome can tolerate leading-strand template lesions and synthesize the leading-strand template discontinuously. However, the single *E. coli* DNA polymerase alone cannot bypass this DNA damage. Additionally, polymerases can transiently dissociate upon encountering the CPD lesion and allow repair enzymes or translesion polymerases to repair or bypass this lesion. The helicase–primase complex remains bound to the template DNA and serves to maintain the integrity of the replication fork, directing the reassembled replisome to the correct location.

3.3 The T4 DNA Replisome Bypassing DNA Damage

Bypass of a noncoding abasic site lesion in either a leading- or lagging-strand template has been studied by T4 DNA replisome. Lesion at the lagging strand blocks the lagging-strand DNA polymerase but does not block the helicase, primase, or leading-strand polymerase. When the primase synthesizes another RNA primer and the clamp is loaded, the stalled lagging-strand polymerase recycles from the DNA lesion and initiates the synthesis of a new Okazaki fragment. Therefore, this lesion does not affect the movement of the DNA replisome, with only a ssDNA gap left behind. In contrast, when a blocking lesion is at the leading-strand template, the leading-strand polymerase is blocked, but the bound helicase continues to travel, causing the leading-strand template to loop out. The leading-strand template is then rapidly coated with ssDNA binding protein. The replication fork travels about 1 kb beyond the DNA lesion before the replication fork completely collapses. The primase and lagging-strand polymerase remain active, and Okazaki fragments are synthesized beyond the leading-strand lesion.

Single-molecule magnetic tweezers were used to study the mechanism of restarting the T4 replication fork that has been blocked by blocked DNA. The T4 DNA holoenzyme, in cooperation with UvsW helicase, can overcome a leading-strand lesion by periodical formation and migration of a four-way Holliday junction. The initiation of the repair process requires partial disassembly of the replisome through the departure of the replicative helicase. With the assistance of other accessory proteins, T4 DNA holoenzyme can bypass this leading-strand lesion.

3.4 The T7 DNA Replisome Bypassing DNA Damage

Single-phosphodiester bond interruptions (nicks) can be introduced by endonucleases, recombination, repair, and the presence of two adjacent Okazaki fragments. Either T7 helicase or DNA polymerase alone was blocked upon encountering a nick in duplex DNA. However, the helicase–polymerase complex can bypass this nick. In dsDNA unwinding, helicase contacts both DNA strands. However, a nick does not provide these contacts, and the helicase itself cannot unwind a nick. When helicase is associated with a DNA polymerase, protein interactions allow the helicase to bind to the template and to encircle helicase onto the 5′-end ssDNA of a nick, thus bypassing the nick. Addition of ssDNA binding protein gp2.5 to the complex further facilitates nick bypass by ~twofold.

Without ssDNA binding protein gp2.5, helicase and DNA polymerase cannot initiate strand-displacement DNA synthesis from a nick. Gp2.5 can bind to the displaced ssDNA, and its acidic C-terminal tail can interact with DNA polymerase. The helicase replaces gp2.5 and catalyzes strand-displacement DNA synthesis with gp5/trx at this nick. Therefore, protein interactions within the T7 DNA replisome may alter the ability of the DNA polymerase to bypass DNA damage and may produce completely different results from those obtained from isolated T7 DNA polymerase (or the trx complex).

Further Reading

Zhang H, Lee SJ, Richardson CC (2011) Essential protein interactions within the replisome regulate DNA replication. Cell Cycle 10:3413–3414

Cox MM, Goodman MF, Kreuzer KN, Sherratt DJ, Sandler SJ, Marians KJ (2000) The importance of repairing stalled replication forks. Nature 404:37–41

Zhang H, Lee SJ, Zhu B, Tran NQ, Tabor S, Richardson CC (2011) Helicase-DNA polymerase interaction is critical to initiate leading-strand DNA synthesis. Proc Natl Acad Sci USA 108:9372–9377

Tabor S, Huber HE, Richardson CC (1987) Escherichia-Coli Thioredoxin Confers Processivity on the DNA-Polymerase-Activity of the Gene-5 Protein of Bacteriophage-T7. J Biol Chem 262:16212–16223

Marintcheva B, Hamdan SM, Lee SJ, Richardson CC (2006) Essential residues in the C terminus of the bacteriophage T7 gene 2.5 single-stranded DNA-binding protein. J Biol Chem 281:25831–25840

Kuzminov A (1995) Collapse and repair of replication forks in Escherichia coli. Mol Microbio 16:373–384

Zhu B, Lee SJ, Richardson CC (2011) Bypass of a nick by the replisome of bacteriophage T7. J Biol Chem 286:28488–28497

Kaplan DL (2000) The 3′-tail of a forked-duplex sterically determines whether one or two DNA strands pass through the central channel of a replication-fork helicase. J Mol Biol 301:285–299

Ghosh S, Marintcheva B, Takahashi M, Richardson CC (2009) C-terminal Phenylalanine of Bacteriophage T7 Single-stranded DNA-binding Protein Is Essential for Strand Displacement Synthesis by T7 DNA Polymerase at a Nick in DNA. J Biol Chem 284:30339–30349

Hamdan SM, Richardson CC (2009) Motors, Switches, and Contacts in the Replisome. Annu Rev Biochem 78:205–243

McInerney P, Donnell MO (2007) Replisome fate upon encountering a leading strand block and clearance from DNA by recombination proteins. J Biol Chem 282:25903–25916

McInerney P, Donnell MO (2004) Functional uncoupling of twin polymerases - Mechanism of polymerase dissociation from a lagging-strand block. J Biol Chem 279:21543–21551

Yeeles JTP, Marians KJ (2011) The Escherichia coli Replisome Is Inherently DNA Damage Tolerant. Science 334:235–238

Jeiranian HA, Schalow BJ, Courcelle CT, Courcelle J (2013) Fate of the replisome following arrest by UV-induced DNA damage in Escherichia coli. Proc Natl Acad Sci USA 110:11421–11426

Nelson SW, Benkovic SJ (2010) Response of the Bacteriophage T4 Replisome to Noncoding Lesions and Regression of a Stalled Replication Fork. J Mol Biol 401:743–756

Manosas M, Perumal SK, Croquette V, Benkovic SJ (2012) Direct Observation of Stalled Fork Restart via Fork Regression in the T4 Replication System. Science 338:1217–1220

Chapter 4
External Causes for DNA Damage

Abstract Various environmental carcinogens may harm human health. Environmental carcinogens damage genome by forming DNA adducts through different chemical reactions, including alkylation (which may involve cross-linking), oxidation, deamination, coordination, photo-addition, and hydrolysis. The DNA damage further results in various disease, cancer, and tumor.

Keywords Environmental carcinogens · DNA adduct · Chemical reactions · Alkylation · Oxidation · Deamination

4.1 Environmental Carcinogens

Large amounts of chemicals are produced in industry, chemical engineering, agriculture, and exhaust. These environmental chemicals can be widely spread in air, water, and soil. Many of them have been shown to cause cancer (termed carcinogens). Animals produced tumors after exposure to these environmental carcinogens. Human exposure to specific chemical or physical carcinogens also produces characteristic mutational spectra, considered to be relevant to including tumor, cancer, and aging. Therefore, studies on how carcinogens lead to various diseases have been received world-wide attention.

4.2 Formation of DNA Damage After Exposure to Environmental Carcinogens

Environmental carcinogens result in DNA adducts through alkylation, amination, oxidation, photo-addition, hydrolysis, and coordination. Alkylating agents produce N^2-alkyl-2′-deoxyguanosine (N^2-alkylG), O^6-alkyl-2′-deoxyguanosine (O^6-alkylG), polycyclic aromatic hydrocarbon modified DNA adducts (PAH-DNA),

H. Zhang, *DNA Replication - Damage from Environmental Carcinogens*,
SpringerBriefs in Biochemistry and Molecular Biology 17,
DOI 10.1007/978-94-017-7212-9_4

and etheno (ε) DNA adducts. Bis-electrophilic agents form DNA–DNA or DNA–protein cross-links. Oxidizing agents, ionizing radiation, and UV irradiation can form 7,8-dihydro-8-oxo-2′-deoxyguanosine (8-oxoG). Arylamines and 1-nitropyrene (1-NP) produce 2-aminofluorene (AF-dG) and *N*-[deoxyguanosine-8-yl]-1-aminopyrene (APG) following oxidation and esterification. UV radiation leads to photoproducts (cyclobutane pyrimidine dimer, CPD). Spontaneous hydrolysis of nucleotides results in the formation of apurinic/apyrimidinic (AP) sites. Heavy metal ions, e.g., Cr(III), form DNA–DNA or DNA–protein cross-links by coordination.

Alkylation: Formaldehyde reacts with the exocyclic amino group of G to produce N^2-methylG (Fig. 4.1). Ethanol is enzymatically oxidized to acetaldehyde, which forms N^2-ethylG (Fig. 4.1), present in liver DNA and urine of alcoholic patients. During these reactions, the intermediate imine is reduced to balance the stoichiometry. Acrolein forms 1,N^2-propano-2′-deoxyguanosine (1,N^2-propanoG) (a ring-opened aldehyde) by the reaction of the amino group at C2 position of deoxyguanosine with the double bond of acrolein. The aldehyde group can further reversely react with the N1 atom of deoxyguanosine to form a ring-closed form, a hemiaminal.

O^6-methylG (O^6-MeG, Fig. 4.1) is a common lesion arising from methylation at the oxygen atom at C6 position of G after exposure to tobacco-specific nitrosamines. Many methylating agents are used in chemotherapy, in which this DNA adduct was also produced. O^6-BenzylG, N^2-benzylG, and N^6-benzylA (Fig. 4.1)

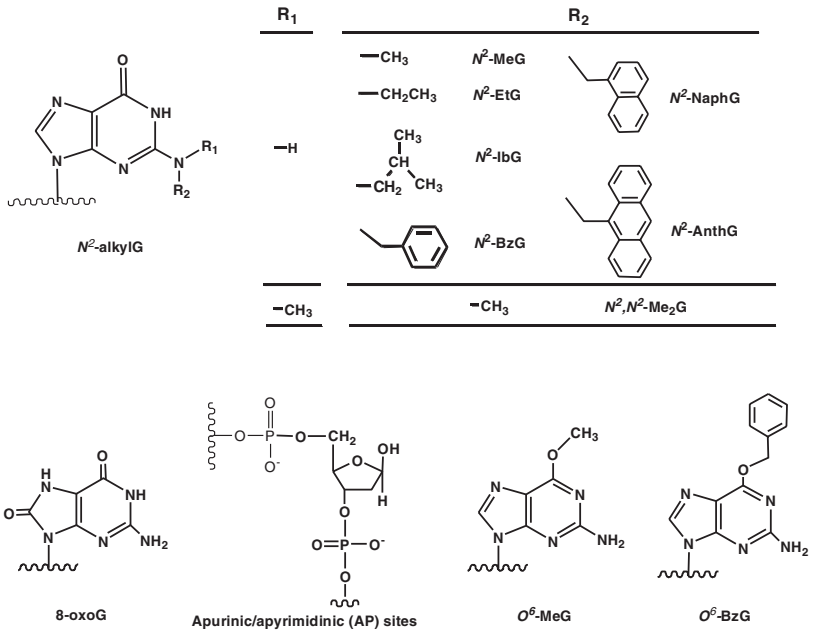

Fig. 4.1 Structures of some typical DNA damage

can be formed by benzylation at the oxygen atom at C6 position or exocyclic amino group at the N2 position of deoxyguanosine or the amino group at the N6 position of adenosine, respectively, after exposure to benzyl chloride.

Lipid peroxidation and exposure to bioactivated carcinogens vinyl chloride and vinyl carbamate can lead to the formation of a series of exocyclic etheno (ε) DNA adducts, including 1,N^6-ethenoadenine (1,N^6-εA), 3,N^4-ethenocytidine (3,N^4-εC), N^2,3-ethenoguanine (N^2,3-εG), and 1,N^2 ethenoguanine (1,N^2-εG). Alkylation of DNA by the reactive products of polycyclic aromatic hydrocarbons (PAHs) can also form PAH-DNA adducts. For example, benzo[*a*]pyrene (B[*a*]P) is initially oxidized to an epoxide (B[*a*]P-7,8-epoxide), then hydrolyzed to a dihydrodiol (B[*a*]P-7,8-dihydrodiol), and further converted to a diol-epoxide (B[*a*]P-7,8-dihydrodiol-9,10-epoxide, BPDE), which alkylates the exocyclic amino group at the N2 position of G or the N7 position of A to form BPDE–DNA adducts.

Amination: Arylamines and *N*-acetyl arylamines are carcinogens found in numerous occupational settings, tobacco smoke, and chemical dyes, leading to 2-aminofluorene (AF-dG) and *N*-acetyl-2-aminofluorene (AAF-dG) through amination of the C8 atom of guanine (via an initial N7 reaction, linking the amine group of the arylamine). 1-Nitropyrene (1-NP) is the most abundant nitrated PAH. The active product of 1-NP (an ester of the reduction product hydroxylamine) forms a bulky *N*-[deoxyguanosine-8-yl]-1-aminopyrene (APG) adduct by reaction at the C8 atom of deoxyguanosine.

Oxidation: Oxidizing agents can produce 7,8-dihydro-8-oxodeoxyguanosine (8-oxoG) lesions (Fig. 4.1). 8-oxoG is a ubiquitous lesion arising from the oxidation of C8 atom of G to form a hydroxyl group by free radical intermediates of oxygen, which are produced by chemical oxidation, ionizing radiation, or UV irradiation. The enol (a lactim) at the C8-N7 position of G is converted to a more stable 8-oxoG lactam form.

Photo-addition: UV radiation can lead to the formation of photoproducts, CPD, by cycloaddition of the C5–C6 double bonds of adjacent pyrimidine bases. Six diastereomers are generated in photo-addition, dependent on the position of pyrimidine moieties with respect to the cyclobutane ring (*cis*/*trans* stereochemistry) and on the relative orientation of the two C5–C6 bonds (*syn*/*anti* regiochemistry. The *trans-anti* and *trans-syn* photoproducts are only present within single-strand or denatured DNA. The *cis-syn* form is formed in large excess relative to the *trans-syn* diastereomers within dsDNA.

Hydrolysis: Abasic sites (referred as AP sites) (Fig. 4.1) lose genetic information. AP sites are generated via spontaneous, chemically induced, or enzyme-catalyzed hydrolysis of the *N*-glycosyl bond. In mammalian cells, approximately 12,000 purines would be spontaneously lost per genome per cell generation (20 h) without protective effects of chromatin packaging. Depyrimidination occurs at a rate about 100 times slower than depurination. Damaging chemicals, e.g., free radicals and alkylating agents, also promote base release, mostly by modifying base structures that destabilize the *N*-glycosyl linkage to generate positively charged leaving groups.

Coordination: Heavy metal ions can form DNA–DNA inter-strand or intra-strand cross-links by coordination interactions. Cr (VI) complexes can permeate cell membranes, in which Cr (VI) is reduced to Cr (III). Cr (III) can coordinate with oxygen atoms of phosphate backbone of two adjacent nucleotides in one or two adjacent DNA strands, producing Cr (III)–DNA intra-strand or inter-strand cross-links.

4.3 Disease, Cancer, and Tumor Resulted from Environmental Carcinogens

Yamagiwa and Ishikawa reported in 1915 the formation of tumors in the ears of rabbits after treatment with tars, and Cook et al. in 1933 isolated benzo[*a*]pyrene as a carcinogenic component of coal tar. Till now, many chemicals have been shown to cause cancer (termed carcinogens). Animals produce tumors after exposure to many environmental carcinogens. Human exposure to specific chemical or physical carcinogens also produces characteristic mutational spectra, including tumor, cancer, and aging. Therefore, studies on how carcinogens lead to cancer have received great attention.

Environmental carcinogens can be converted to reactive products in the body. These intermediates react with DNA to form DNA carcinogen adducts. In each human cell, >50,000 DNA-damaging events can occur every day. One cause of human breast cancer is that TP53 and MYC expressing endogenously high levels of APOBEC3B lead C to T point mutation in somatic cells. DNA adducts lead to mutations in DNA replication, resulting in cell necrosis, aging, tumor, and cancer. DNA replication can produce mutations and directly lead to human diseases. Mutations or defects in human pol η result in one form of xeroderma pigmentosum V (XP-5), mutations of human pol β are associated with adenocarcinoma of the colon, and mutations of human pol γ result in progressive external ophthalmoplegia.

Further Reading

Yamagiwa K, Ichikawa K (1915) Experimentelle studie über die pathogenese der epithelialgeschwülste. Mitt Med Fak Tokio 15:295–344

Cook JW, Hewett CL, Hieger I (1933) The isolation of a cancer-producing hydrocarbon from coal tar Parts I, II, and III. J Chem Soc 106:395–405

Bechtel DH (1989) Molecular dosimetry of hepatic aflatoxin B_1-DNA adducts: linear correlation with hepatic cancer risk, Regulatory Toxicology and Pharmacology. Regul Toxicol Pharmacol 10:74–81

Hsu IC, Metcalf RA, Sun T, Welsh JA, Wang NJ, Harris CC (1991) Mutational hot spot in the p53 gene in human hepatocellular carcinomas. Nature 350:427–428

K.H. Vahakangas, J.M. Samet, R.A. Metcalf, J.A. Welsh, W.P. Bennett, D.P. Lane, C.C. Harris, Mutations of p53 and ras genes in radon-associated lung cancer from uranium miners, Lancet, 339 (1992) 576–580

Denissenko MF, Pao A, Tang M, Pfeifer GP (1996) Preferential formation of benzo[*a*]pyrene adducts at lung cancer mutational hotspots in *P53*. Science 274:430–432

Guengerich FP (2006) Interactions of carcinogen-bound DNA with individual DNA polymerases. Chem Rev 106:420–452

Yasui M, Matsui S, Ihara M, Laxmi YR, Shibutani S, Matsuda T (2001) Translesional synthesis on a DNA template containing N^2-methyl-2'-deoxyguanosine catalyzed by the Klenow fragment of Escherichia coli DNA polymerase I. Nucl Acids Res 29:1994–2001

Cheng TF, Hu XP, Gnatt A, Brooks PJ (2008) Differential blocking effects of the acetaldehyde-derived DNA lesion N-2-ethyl-2'-deoxyguanosine on transcription by multisubunit and single subunit RNA polymerases. J Biol Chem 283:27820–27828

Brooks PJ, Theruvathu JA (2005) DNA adducts from acetaldehyde: implications for alcohol-related carcinogenesis. Alcohol 35:187–193

Georgiadis P, Samoli E, Kaila S, Katsouyanni K, Kyrtopoulos SA (2000) Ubiquitous presence of O^6-methylguanine in human peripheral and cord blood DNA. Cancer Epidemiol Biomarkers Prev 9:299–305

Margison GP, Koref MFS, Povey AC (2002) Mechanisms of carcinogenicity/chemotherapy by O^6-methylguanine. Mutagenesis 17:483–487

Uziel M, Munro NB, Katz DS, Vo-Dinh T, Zeighami EA, Waters MD, Griffith JD (1992) DNA adduct formation by 12 chemicals with populations potentially suitable for molecular epidemiological studies. Mutat Res 277:35–90

Cheng SC, Hilton BD, Roman JM, Dipple A (1989) DNA adducts from carcinogenic and noncarcinogenic enantiomers of benzo[a]pyrene dihydrodiol epoxide. Chem Res Toxicol 2:334–340

Zhao L, Pence MG, Christov PP, Wawrzak Z, Choi JY, Rizzo CJ, Egli M, Guengerich FP (2012) Basis of Miscoding of the DNA Adduct N^2,3-Ethenoguanine by Human Y-family DNA Polymerases. J Biol Chem 287:35516–35526

Lawley P, Brookes P (1967) Interstrand cross-linking of DNA by difunctional alkylating agents. J Mol Biol 25:143–160

Michaelson-Richie ED, Loeber RL, Codreanu SG, Ming X, Liebler DC, Campbell C, Tretyakova NY (2010) DNA-Protein Cross-Linking by 1,2,3,4-Diepoxybutane. J Proteome Res 9:4356–4367

Jelitto B, Vangala R, Laib R (1989) Biological Monitoring of Exposure and the Response at the Subcellular Level to Toxic Substances. Springer 246–249

Nath RG, Ocando JE, Guttenplan JB, Chung FL (1998) I,N^2-propanodeoxyguanosine adducts: potential new biomarkers of smoking-induced DNA damage in human oral tissue. Cancer Res 58:581–584

Stone MP, Cho YJ, Huang H, Kim HY, Kozekov ID, Kozekova A, Wang H, Minko IG, Lloyd RS, Harris TM, Rizzo CJ (2008) Interstrand DNA cross-links induced by alpha,beta-unsaturated aldehydes derived from lipid peroxidation and environmental sources. Acc Chem Res 41:793–804

Degan P, Shigenaga MK, Park EM, Alperin PE, Ames BN (1991) Immunoaffinity isolation of urinary 8-hydroxy-2-deoxyguanosine and 8-hydroxyguanine and quantitation of 8-hydroxy-2'-deoxyguanosine in DNA by polyclonal antibodies. Carcinogenesis 12:865–871

Fraga CG, Shigenaga MK, Park JW, Degan P, Ames BN (1990) Oxidative damage to DNA during aging: 8-hydroxy-2'-deoxyguanosine in rat organ DNA and urine. Proc Natl Acad Sci USA 87:4533–4537

Vrtis KB, Markiewicz RP, Romano LJ, Rueda D (2013) Carcinogenic adducts induce distinct DNA polymerase binding orientations. Nucleic Acids Res 41:7843–7853

Kirouac KN, Basu AK, Ling H (2013) Structural Mechanism of Replication Stalling on a Bulky Amino-Polycyclic Aromatic Hydrocarbon DNA Adduct by a Y Family DNA Polymerase. J Mol Biol 425:4167–4176

O'Brien T, Mandel HG, Pritchard DE, Patierno SR (2002) Critical role of chromium (Cr)-DNA interactions in the formation of Cr-induced polymerase arresting lesions. Biochemistry 41:12529–12537

Cadet J, Voituriez L, Hruska FE, Kan LS, Leeuw FAd, Altona C (1985) Characterization of thymidine ultraviolet photoproducts. Cyclobutane dimers and 5, 6-dihydrothymidines. Can J Chem 63:2861–2868

Ravanat JL, Douki T, Cadet J (2001) Direct and indirect effects of UV radiation on DNA and its components. J Photoch Photobio B 63:88–102

Wilson III DM, Barsky D (2001) The major human abasic endonuclease: formation, consequences and repair of abasic lesions in DNA. Mutat Res-DNA Repair 485:283–307

Ling H, Boudsocq F, Woodgate R, Yang W (2001) Crystal structure of a Y-family DNA polymerase in action: a mechanism for error-prone and lesion-bypass replication. Cell 107:91–102

Chapter 5
Effect of Environmental Carcinogens on Cellular Physiology

Abstract Environmental carcinogens affect cell cycle progression, proliferation, differentiation, DNA replication and repair, apoptotic pathways, and tissue pathology. Carcinogens regulate cell cycle by activation of some cellular signal pathways or formation of DNA damage. Carcinogens also induce cell apoptosis through different manners and promote cell proliferation through the inhibition of cell apoptosis. Gene expression is affected by carcinogens mainly through the activation of signaling pathways and interaction with cellular DNA.

Keywords Environmental carcinogens · Cell cycle progression · Proliferation · Differentiation · Apoptotic · Tissue pathology

5.1 Overview of Biological Activities of Cells

Cell is the basic structural and function unit of life, and it is highly complicated and organized, self-regulated. Cells consist of protoplasm enclosed within a membrane, which contains many biomolecules such as proteins and nucleic acids. The biological activities of cell mainly include growth, metabolism, proliferation, apoptosis, and senescence. Cells grow through the functioning cellular metabolism, by which individual cells process nutrient molecules. Cell proliferation refers to cell produce themselves by division. A single cell (called a mother cell) is divided into two daughter cells, which involves a serial of highly regulated events that lead to DNA replication and cell division. Apoptosis is the process of programmed cell death, which leads to characteristic cell changes and death. These changes include blebbing, cell shrinkage, nuclear fragmentation, chromatin condensation, and chromosomal DNA fragmentation. Apoptosis is a normal physiologic process and plays an important role in homeostasis and development of the tissue. Cell senescence is the gradual deterioration of function characteristic of cell, for example, normal diploid cells cease to divide, normally after about 50 cell divisions in vitro.

H. Zhang, *DNA Replication - Damage from Environmental Carcinogens*,
SpringerBriefs in Biochemistry and Molecular Biology 17,
DOI 10.1007/978-94-017-7212-9_5

Environmental carcinogens have multiple effects on cells, including effects on cell cycle progression, proliferation, differentiation, DNA replication and repair, as well as apoptotic pathways.

5.2 Cell Cycle

Cell cycle is a set of event responsible for cell duplication. Cell cycle is divided into four phases. Transmission of genetic information from one cell generation to the next requires DNA replication during the S phase, and its segregation to the two new daughter cells is happened during M phase. Cell cycle is rigorously ordered for the correct duplication of cell. In a cell cycle, S phase is preceded by M phase does not occur until S phase is completed. The time and order of cell cycle event are monitored by cell cycle checkpoints that occur at the G1/S boundary, in S phase, and during G2/M phase. The checkpoints enable correct duplication of cell. If something wrong is happened in the process of cell cycle, the checkpoints will be activated.

Environmental carcinogens can regulate cell cycle by activation of some cellular signal pathways or formation of DNA damage. Environmental carcinogens affect cell cycle mainly through acceleration or arrest of cell cycle progression, which is mediated by sequential activation and inactivation of Cdks, a family of serine/threonine protein kinases. These kinase activities are depended on cyclins. 2-Methoxy-4-vinylphenol, an aromatic substance used as a flavoring agent, induces cell cycle arrest in G1 phase because of the increased expression of CDK inhibitor, p21, and p15; the decreased expression of cyclin D1 and cyclin E; and the inhibited kinase activities of CDK4 and CDK2. Another potent mammary carcinogen 6-nitrochrysene, increases the protein expression of cyclin-dependent kinase inhibitor p21 and a commitment increase of G1 phase in MCF-10A cells.

In addition, some environmental carcinogens also alter cell cycle due to formation of DNA damage. The cell cycle checkpoints can be activated by DNA damage. Once activated, cell progression is stopped, allowing the cell to repair DNA damage. After damage repair, the progression of cell cycle resumes. Ochratoxin A, one of the most abundant food-contaminating mycotoxins, induces the formation of DNA damage and cell cycle arrest in human embryonic kidney cells (Yang et al. 2014). Condurango glycoside-rich component, which is a potential chemotherapeutic agent, stimulates DNA damage-induced cell cycle arrest in lung cancer cells.

Environmental carcinogens can also promote cell cycle progression. Di-(2-ethylbexyl) phthalate, which is persistent organic pollutant, increases DNA replication rate and accelerates the cell cycle through activating PI3 K–AKT–mTOR signaling pathway. Tobacco-specific carcinogen 4-(methylnitrosamino)-1-(3-pyridyl)-1-butanone also promotes cells to enter into the S phase through NFkB activation and cyclin D1 up-regulation.

5.3 Cell Proliferation and Apoptosis

5.3.1 Cell Apoptosis

Cell growth and apoptosis are highly regulated for homeostasis and development of the tissue. Apoptosis is program cell death, which can be initiated via two classical pathways. Binding of death ligands to their corresponding receptors leads to the activation of caspase 8. Disruption of mitochondrial membrane integrity by exogenous substances or endogenous expression of bcl-2 genes leads to the release of mitochondrial pro-apoptotic proteins and the activation of caspase 9. Caspases 8 and 9 further activate executioner caspases 3 and 7, resulting in proteolysis of proteins and cell death.

Apoptosis is the main cell death pathway that environmental carcinogens result in. It has been reported that various kinds of environmental carcinogens can induce cell apoptosis in vitro through different manners. One way is to regulate proteins that are correlated with apoptosis. The family of bcl-2 proteins is correlated with the release of mitochondrial cytochrome c and the activation of caspases. The metabolite of benzo[a]pyrene, B[a]P-7,8-dihydrodiol (BPDE), was found to induce apoptosis in human HepG2 cells, in which the exposure to BPDE initiates the degradation of Bid and the activation of other pro-apoptotic proteins, such as Bak. Simultaneously, BPDE stimulates the inhibition of anti-apoptotic proteins, such as Bcl-xL, which inhibits the release of mitochondrial cytochrome c. Another way is to form DNA damage. Environmental carcinogens can result in DNA lesion, such as DNA adducts and DNA strand break. If the DNA damage cannot be repaired, apoptosis will be activated.

Beside for the above-described manners, oxidative stress also plays an important role in the apoptosis induced by environmental carcinogens. Reactive oxygen species (ROS) are continually generated and eliminated in biological systems and affect normal biochemical functions. Excess production of ROS in the cell induces apoptosis. Abnormal functions result in pathological processes. Highly reactive hydroxyl radicals attack cellular components, such as DNA, lipids, and proteins, to cause various kinds of oxidative damages. Polychlorobiphenyls (PCBs) congeners, PCB-77 and PCB-153, induce oxidative stress that leads to apoptosis in human liver cell line. 3-Nitrobenzanthrone and its main metabolite, 3-aminobenzanthrone, enhances the production of ROS and DNA damage. ROS is generated from mitochondrial and cytochrome P450s when environmental carcinogens induce cell apoptosis. These carcinogens are activated to produce ROS through cytochrome P450s. More importantly, the mitochondrial electron chain is the major source to "accidentally" generate ROS during apoptosis.

5.3.2 Cell Proliferation

In addition to cell apoptosis, environmental carcinogens can also promote cell proliferation, which result in carcinogenesis and aberrant cell accumulation. The promotion of cell proliferation induced by environmental carcinogens is mainly through regulation

of signal transduction pathways. Three major mitogen-activated protein kinase (MAPK) pathways control various cellular processes, including cell proliferation, differentiation, apoptosis, and stress responses to environmental stimuli. Each of the MAPK pathways consists of three-tiered cascades that mediate the signal transduction pathways from a variety of extracellular signals to regulate the expression of specific genes. MAPKs are comprised of three major subfamilies of tyrosine/threonine kinases: (i) the extracellular-signal-regulated kinases (ERK1/2), (ii) the c-jun N-terminal kinases or stress-activated protein kinases (JNK1/2 or SAPK), and (iii) p38 MAPK. Activation of ERK1/2 is mainly involved in cell proliferation and survival, whereas activation of JNK1/2 and p38 MAPK is associated with growth arrest and apoptosis.

Environmental carcinogens can promote cell proliferation by activating ERK1/2 pathways. The strongest tobacco-specific carcinogens 4-(methylnitrosamino)-1-(3-pyridyl)-1-buta-none (NNK) showed a strong proliferative effect on human normal and cancer mammary epithelial cells; the proliferation multitudes of these cells are well correlated with the activation levels of ERK1/2 MAP kinases. Some environmental carcinogens can activate MAPK pathway, while it is dose-dependent. Arsenic is a well-known carcinogen that possibly promotes tumors and the development of various types of cancers. It has been shown that, dependent on the dosage, arsenic can lead to cell proliferation through the ERK or apoptosis through the JNK pathway. A low level (2 μM) of arsenite stimulates extracellular-signal-regulated kinase (ERK) signaling pathway and enhances cell proliferation. In contrast, a high level (40 μM) of arsenite stimulates the c-Jun N-terminal kinase (JNK) signaling pathway and induces cell apoptosis.

Epidermal growth factor receptor (EGFR) signaling pathway also regulates cell proliferation. Epidermal growth factor (EGF) plays an important role in the regulation of cell growth, proliferation, and differentiation. EGF-binding EGFR on the cell surface stimulates the intrinsic protein–tyrosine kinase activity of the receptor and initiates a signal transduction cascade. As a result, intracellular calcium levels are increased, glycolysis and protein synthesis are performed, and some certain genes were transcripted, leading to DNA synthesis and cell proliferation. Benzo[a]pyrene promotes proliferation of human lung cancer cells by enhancing the epidermal growth factor receptor (EGFR) signaling pathway. The possible reason was that benzo[a]pyrene may increase the expression of amphiregulin, one of the ligands of the EGFR.

In addition, environmental carcinogens promote cell proliferation through the inhibition of cell apoptosis. Benzene is a widely recognized human carcinogen. Benzene metabolites, p-benzoquinone and hydroquinone, restrain the NIH3T3 cells apoptosis by inhibition of caspase-3. 2,3,7,8-Tetrachlorodibenzo-p-dioxin (TCDD) is a highly toxic pollutant ubiquitously present in the environment. TCDD causes cancer in multiple tissues in different animal species and is classified as a class 1 human carcinogen. It has been hypothesized that TCDD acts as a tumor promotor by preventing the initiated cells from undergoing apoptosis. TCDD partially inhibits apoptotic DNA fragmentation in both primary rat hepatocytes and Huh-7 human hepatoma cells without affecting upstream apoptotic events (Martin et al. 2009). Survival of apoptosis might be involved in the initiation of some types of cancer.

5.3.3 Gene Expression

Many studies have indicated that the incidence of cell carcinoma is associated with environmental carcinogens and genetic factors. The biological activities of cell are controlled by genes, so the effects of environmental carcinogens on cell are closely related to gene expression. In fact, the effects described above, including cell cycle, cell apoptosis, and cell proliferation, have been involved in gene expression. Several studies showed that environmental carcinogens alter genes that are involved in immune, inflammatory and stress responses and apoptosis. Different carcinogens may induce different gene expression, and gene expression may be dose-dependent. Fifteen genotoxic carcinogens were used to characterize gene expression in human lymphoblastoid cells (TK6 cells), and no similar gene expression was observed among these carcinogens. The gene expression was observed as linear relationship with the dose of trichloroethylene, benz[a]anthracene, epichlorohydrin, benzene, and hydroquinone. The significantly altered genes were involved in the regulation of (anti-) apoptosis, maintenance of cell survival, tumor necrosis factor-related pathways, and immune response. Inorganic arsenic (iAs) is a human urinary bladder, skin, and lung carcinogen. Increasing concentrations of iAs induced more genes and additional signaling pathways in HBE cells. The major signaling pathways altered included NRF2-mediated stress response, interferon, p53, cell cycle regulation, and lipid peroxidation.

Some environmental carcinogens are not directly carcinogenic, but they can convert to reactive metabolites which are capable of interaction with cellular DNA to form DNA adducts. Metabolizing enzymes are required in these processes. Environmental carcinogens can affect the expression of genes of these enzymes. Cytochrome P450s (CYPs), an oxidase system, are involved in the metabolism of exogenous substrates, including benzene, carbon tetrachloride, ethylene glycol, and nitrosamines. CYP1A1 is capable of metabolizing benzo[a]pyrene via an oxidation process. It has shown that benzo[a]pyrene can induce the expression of CYP1A1 gene. CYP2E1 is known to be involved in the metabolism of benzene, and its expression was increased in peripheral blood mononuclear cells even the concentration of benzene in air is as low as 0.01 ppm.

Gene expression is affected by carcinogens mainly through the activation of signaling pathways and interaction with cellular DNA. Mineral dust-induced gene (Mdig), a newly identified oncogene, is linked to occupational lung diseases and lung cancer. Using human bronchial epithelial cells and human lung cancer cell lines, arsenic was found to induce the expression of Mdig, partially dependent on the JNK and STAT3 signaling pathways. In recent years, “omic” technologies, which is a manually curated metadatabase that provides an overview of more than 4400 Web-accessible tools related to genomics, transcriptomics, proteomics, and metabolomics, have been employed to get a deeper understanding of toxicological mechanisms and to predict toxicological outcome, such as carcinogenicity, by profiling genomic perturbations. Toxicogenomic tools have also been utilized to discriminate between classes of carcinogens based on global expression profiling. This

suggests that for compounds with insufficient toxicological information, associated gene signatures could be used to characterize their toxicological properties based on comparison with signatures associated with previously characterized compounds.

5.3.4 Cell and Tissue

Environmental carcinogens affect cellular physiology, including cell cycle progression, proliferation, DNA replication, and gene expression, result in tissue pathology, which refer to disease and carcinoma.

Tobacco-specific nitrosamines (TSNA) have implications in the pathogenesis of various lung diseases, and conditions are prevalent even in non-smokers. *N*-nitrosonornicotine (NNN) and 4-(methyl-nitrosamino)-1-(3-pyridyl)-1-butanone (NNK) are potent pulmonary carcinogens present in tobacco products and are mainly responsible for lung cancer. NNK and NNN significantly enhances phospholipase A2 activity and reduces the surfactant lung phospholipid level. Exposure to carcinogenic polycyclic aromatic hydrocarbons (PAHs) has been implicated as the etiology of atherosclerosis. Monocyte-chemoattractant protein 1 (MCP-1) promotes the recruitment of monocytes into atherosclerotic lesions. Treatment with B[a]P induces MCP-1 gene expression through activation of aryl hydrocarbon receptor in aortic tissue of ApoE−/−mice. These observations are agreed with in vitro studies with human endothelial cells (RF24 cell line and primary HUVEC).

Carcinogens can lead to tissue carcinoma. PAH and TSNA are recognized as potential etiological agents for oral cancer. Dibenzo[a,l]pyrene, the most potent known environmental carcinogen among PAH, is carcinogenic in the oral tissues of mice. Dibenzo[a,l]pyrene induces overexpression of p53 and COX-2 proteins in malignant tissues compared to normal oral tissues and tongues.

The effect of environmental carcinogens on tissue is studied in vivo; however, the molecular mechanism is studied in vitro. In order to further understand the damage effects of environmental carcinogens, we should combine the outcomes in vivo and vitro. Collaborative efforts are still required to investigate the effects of carcinogens on human health and to develop effective assays for toxicity assessment, and to explore the effects of carcinogen on chemical pathways.

Further Reading

Andy Lau TY, Muyao L, Ronglin X, He QY, Chiu JF (2004) Opposed arsenite-induced signaling pathways promote cell proliferation or apoptosis in cultured lung cells. Carcinogenesis 25(1): 21–28

Bruna P, Margaret K, Antonio G (2000) Cell cycle and apoptosis. Neopiasia 2(4): 291–299

Chen S, Nguyen N, Tamura K, Karin M, Tukey RH (2003) The role of the Ah receptor and p38 in benzo[a]pyrene-7, 8-dihydrodiol and benzo[a]pyrene-7, 8-dihydrodiol-9,10-epoxide-induced apoptosis. J Biol Chem 278(21):19526–19533

Chen X, Qin Q, Zhang W, Zhang Y, Zheng H, Liu C, Yuan J (2013) Activation of the PI3 K-AKT-mTOR signaling pathway promotes DEHP-induced Hep3B cell proliferation. Food Chem Toxicol 59: 325–333

Chen ZB, Li C, Chen FQ, Li SY, Liang Q, Liu LY (2006) Effects of tobacco-specific carcinogen 4-(methylnitrosamino)-1-(3-pyridyl)-1-butanone (NNK) on the activation of ERK1/2 MAP kinases and the proliferation of human mammary epithelial cells. Environ Toxicol Phar 22:283–291

Christoph C, Geilen CC, Marcus W, Orfanos C E (1996) The mitogen- activated protein kinases system (MAP kinase cascade)_ its role in skin signal transd. J Dermatol Sci e 12(3): 255–262

Danial NN, Korsmeyer SJ (2004) Cell death: Critical control points. Cell 116(2): 205–219

De S, Ghosh S, Chatterjee R, Chen YQ, Moses L, Kesari A, Dutta SK (2010) PCB congener specific oxidative stress response by microarray analysis using human liver cell line. Environ Int 36(8):907–917

Dodmane PR, Arnold LL, Kakiuchi KS, Qiu F, Liu X, Rennard SI, Cohen SM (2013) Cytotoxicity and gene expression changes induced by inorganic and organic trivalent arsenicals in human cells. Toxicology 312:18–29

Dunn KL, Espino PS, Drobic B, He S, Davie JR (2005) The Ras-MAPK signal transduction pathway, cancer and chromatin remodeling. Biochem Cell Biol 83(1):1–14

Ellinger ZH, Stuart B, Wahle B, Bomann W, Ahr HJ (2005) Comparison of the expression profilesinduced by genotoxic and nongenotoxic carcinogens in rat liver. Mutat Res-Fund Mol M 575(1-2):61–84

Hansen T, Seidel A, Borlak J (2007) The environmental carcinogen 3-nitrobenzanthrone and its main metabolite 3-aminobenzanthrone enhance formation of reactive oxygen intermediates in human A549 lung epithelial cells. Toxicol Appl Pharmacol 221(2): 222–234

Ho YS, Chen CH, Wang YJ, Pestell RG, Albanese C, Chen RJ, Wu CH (2005) Tobacco-specific carcinogen 4-(methylnitrosamino)-1-(3-pyridyl)-1-butanone (NNK) induces cell proliferation in normal human bronchial epithelial cells through NFkB activation and cyclin D1 up-regulation. Toxicol Appl Pharm 205(2):133–148

Jeong JB, Jeong HJ (2010) 2-Methoxy-4-vinylphenol can induce cell cycle arrest by blocking the hyper-phosphorylation of retinoblastoma protein in benzo[a]pyrene-treated NIH3T3 cells. Biochem Bioph Res Co 400(4):752–757

Knaapen AM, Curfs DeM, Pachen DeM, Gottschalk RW, Winther MPJd, Daemen MJ, Schooten FJV (2007) The environmental carcinogen benzo[a]pyrene induces expression of monocyte-chemoattractant protein-1 in vascular tissue: a possible role in atherogenesis. Mutat Res 621(2007):31–41

Ma C, Song M, Zhang Y, Yan M, Zhang M, Bi H (2014) Nickel nanowires induce cell cycle arrest and apoptosis by generation of reactive oxygen species in HeLa cells. Toxicol Reports 1:114–121

Mai Z, Liu H (2009) Boolean network-based analysis of the apoptosis network: irreversible apoptosis and stable surviving. J Theor Biol 259(4):760–769

Malik MA, Upadhyay R, Mittal RD, Zargar SA, Mittal B (2010) Association of Xenobiotic Metabolizing Enzymes Genetic Polymorphisms With Esophageal Cancer in Kashmir Valley and Influence of Environmental Factors. Nutr Cancer 62(6):734–742

Martin C, Arunasalam MD, Meiss G, Schrenk D (2009) Inhibition of UV-C light-induced apoptosis in liver cells by 2,3,7,8-tetrachlorodibenzo-p-dioxin. Toxicol Sci 111(1): 49–63

Roos WP, Kaina B (2006) DNA damage-induced cell death by apoptosis. Trends Mol Med 12(9):440–450

Santen RJ, Song RX, McPherson R, Kumar R, Adam L, Jeng MH, Yue W (2002) The role of mitogen-activated protein (MAP) kinase in breast cancer. J Steroid Biochem Mol Biol 80(2):239–256

Sikdar S, Mukherjee A, Ghosh S, Khuda-Bukhsh AR (2014) Condurango glycoside-rich components stimulate DNA damage-induced cell cycle arrest and ROS-mediated caspase-3 dependent apoptosis through inhibition of cell-proliferation in lung cancer, in vitro and in vivo. Environ Toxicol Phar 37(1):300–314

Sun YW, Herzog CR, Krzeminski J, Amin S, Perdew G, El-Bayoumy K (2007) Effects of the environmental mammary carcinogen 6-nitrochrysene on p53 and p21(Cip1) protein expression and cell cycle regulation in MCF-7 and MCF-10A cells. Chem Biol Interact 170(1):31–39

Kometani T, Yoshino I, Miura N, Okazaki H, Ohba T, Tomoyoshi T, Maehara Y (2009) Benzo[a] pyrene promotes proliferation of human lung cancer cells by accelerating the epidermal growth factor receptor signaling pathway. Cancer Lett 278:27–33

Thomas RS, Allen BC, Nong A, Yang L, Bermudez E, Clewell HJ, Andersen ME (2007) A method to integrate benchmark dose estimates with genomic data to assess the functional effects of chemical exposure. Toxicol Sci 98(1):240–248

Vaughan AT, Betti CJ, Villalobos MJ (2002) Surviving apoptosis. Apoptosis 7(2):173–177

Waters MD, Jackson M, Lea I (2010) Characterizing and predicting carcinogenicity and mode of action using conventional and toxicogenomics methods. Mutat Res-Rev Mutat 705(3):184–200

Weihua Z, Tsan R, Huang WC, Wu Q, Chiu CH, Fidler IJ, Hung MC (2008) Survival of cancer cells is maintained by EGFR independent of its kinase activity. Cancer Cell 13(5):385–393

Yang Q, He X, Li X, Xu W, Luo Y, Yang X, Huang K (2014) DNA damage and S phase arrest induced by Ochratoxin A in human embryonic kidney cells (HEK 293). Mutat Res-Fund Mol M 765:22–31

Chapter 6
Protocols for Studies of Bypass of DNA Damage by DNA Polymerase

Abstract In this chapter, we gave the detailed protocols for studies of bypassing DNA damage using a DNA polymerase. These methods include kinetic analysis, LC-MS/MS sequence analysis of full-length extension products beyond DNA damage, and X-ray crystal structure analysis of DNA polymerase containing DNA damage. Kinetic analysis contains steady-state kinetic analysis of single dNTP incorporation against DNA damage, full-length extension beyond DNA damage, pre-steady-state kinetic analysis of dNTP incorporation, and kinetic analysis of conformational change. This analysis gave details about how a DNA polymerase bypasses DNA damage.

Keywords Steady state · Full-length extension · Pre-steady state · LC-MS/MS sequence analysis · Conformational change · X-ray crystal structure

6.1 Introduction

In order to understand how DNA polymerase to bypass DNA damage, the steady-state kinetic analysis of single dNTP incorporation against DNA damage should be performed to understand how the DNA damage affect dNTP incorporation. Comparison with unmodified nucleotide, we can know how the DNA damage affects DNA replication. The full-length extension beyond DNA damage can tell us how the DNA damage blocks DNA replication. For the details in dNTP incorporation mechanism, pre-steady-state kinetic analysis of dNTP incorporation can discover whether this incorporation has a fast burst phase and what are the dNTP dissociation constant and maximal dNTP incorporation rate. Kinetic analysis of conformational change will discover whether the DNA damage affects the conformational change that is always present for the bypass of unmodified nucleotide. Generally, full-length extension assay cannot give the exact sequence information of the extension products. LC-MS/MS sequence analysis will give the exact sequence information for the full-length extension products beyond DNA damage. Not only kinetic analysis, X-ray crystal structure analysis of DNA polymerase with DNA containing

H. Zhang, *DNA Replication - Damage from Environmental Carcinogens*,
SpringerBriefs in Biochemistry and Molecular Biology 17,
DOI 10.1007/978-94-017-7212-9_6

DNA damage will discover the active-site information in which how DNA damage is aligned and how DNA damage distorts active site. This kinetic analysis and structure analysis gave details about how a DNA polymerase bypasses DNA damage.

6.2 Kinetic Analysis of Bypass of DNA Damage

6.2.1 Materials

The materials were as follows: DNA polymerase, damaged and undamaged ssDNAs, Tris-HCl buffer (pH 7.5), NaCl, dithiothreitol, bovine serum albumin, glycerol, T4 polynucleotide kinase, [γ-^{32}P]ATP, dNTP, $MgCl_2$, EDTA, formamide, bromphenol blue, xylene cyanol, acrylamide, and urea.

6.2.2 Preparation of Reaction Buffer

Reaction buffer contains 50 mM Tris-HCl buffer (pH 7.5) containing 50 mM NaCl, 5 mM dithiothreitol, 100 μg bovine serum albumin ml^{-1} (w/v), and 5 % glycerol (v/v).

6.2.3 Preparation of Reaction Quench Buffer

Reaction quench buffer contains 20 mM EDTA in 95 % formamide (v/v) with 0.5 % bromphenol blue (w/v) and 0.05 % xylene cyanol (w/v).

6.2.4 Preparation of Primer/Template that Contains DNA Damage at Incorporation Position

ssDNA primer was 5′ end-labeled using T4 polynucleotide kinase/[γ-^{32}P]ATP for 30 min at 37 °C. After heating at 95 °C for 10 min to activate T4 polynucleotide kinase, the solution was passed through Bio-Spin-6 (Bio-rad) to remove the unreacted [γ-^{32}P]ATP. Then, the 32P-labeled primer is annealed to templates (20 % molar excess) by heating to 95 °C for 5 min and then slowly cooling to room temperature.

6.2.5 Analysis of DNA Incorporation Product

Products were separated using a 20 % polyacrylamide (w/v) denaturing gel electrophoresis system containing 8 M urea, visualized using a Bio-Rad Molecular Imager FX instrument (Bio-Rad), and quantitated by phosphorimaging analysis using the Molecular Imager FX instrument with Quantity One software.

6.2.6 Primer Extension Assay with All Four dNTPs

^{32}P-labeled DNA substrate (100 nM) was incubated with DNA polymerase (0, 0.5, 2, 10, or 50 nM) in reaction buffer, and reactions were initiated by adding dNTP·Mg^{2+} solution (100 μM each dNTP and 10 mM $MgCl_2$). After different reaction times, the reactions were quenched by quench buffer and analyzed by gel electrophoresis and phosphorimaging.

6.2.7 Steady-State Kinetic Analyses

^{32}P-labeled DNA substrate was extended in the presence of varying concentrations of a single dNTP. The molar ratio of primer/template complex to DNA polymerase is generally ≥10:1. Polymerase concentrations and reaction times were adjusted to limit primer conversion to <20 %. Under this condition, reactions were done with twelve different dNTP concentrations, quenched by the addition of quench buffer, and analyzed by gel electrophoresis. Graphs of product formation rate versus dNTP concentration were fit using nonlinear regression (hyperbolic fits, Eq. 6.1) in GraphPad Prism Version 3.0 (San Diego, CA) for the estimation of k_{cat} and K_m values

$$k_{obs} = k_{cat}[\text{dNTP}]/([\text{dNTP}] + K_m), \tag{6.1}$$

where k_{obs} is the dNTP incorporation rate by unit DNA polymerase, equal to product concentration divided by reaction time and DNA polymerase concentration, [dNTP] is the concentration of dNTP, k_{cat} is the steady-state rate maximal incorporation rate, and K_m is dNTP concentration at half maximal rate.

6.2.8 Pre-steady-state Reactions

Rapid chemical quench experiments were performed using a model RQF-3 KinTek Quench Flow Apparatus (KinTek Corp., Austin, TX) with 50 mM Tris-HCl buffer (pH 7.4) in the drive syringes. Reactions were initiated by rapid mixing of ^{32}P-primer/template and DNA polymerase mixtures with the dNTP·Mg^{2+} complex and then quenched with 0.6 M EDTA after varying reaction times. The reaction products (20 μl) were mixed with 5 μl quench buffer, separated using denaturing gel electrophoresis, and quantitated. Pre-steady-state experiments with excess DNA or with excess DNA polymerase were fit with Eqs. 6.2 and 6.3, respectively, using nonlinear regression analysis in GraphPad Prism Version 3.0,

$$y = A\left(1 - \exp\left(-k_p t\right)\right) + k_{ss} t \tag{6.2}$$

$$y = A\left(1 - \exp\left(-k_p t\right)\right), \tag{6.3}$$

where y is the concentration of product, A is the burst amplitude, k_p is the pre-steady-state rate of nucleotide incorporation, t is time, and k_{ss} is a steady-state velocity of nucleotide incorporation.

k_{pol} and $K_{d,dCTP}$ were estimated by performing pre-steady-state reactions at different dNTP concentrations and varying reaction times. Graphs of burst rates (k_{obs}) versus dNTP concentration were fit to the hyperbolic equation

$$k_{obs} = k_{pol}[dNTP] / \left([dNTP] + K_{d,dCTP}\right) \tag{6.4}$$

where k_{pol} is the maximal rate of nucleotide incorporation, and $K_{d,dCTP}$ is the equilibrium dissociation constant for dNTP.

6.2.9 Pre-steady-state Trap Experiments

In order to test whether the presence of DNA damage accelerates the dissociation of DNA from DNA polymerase, trap assay was performed. Reactions were initiated by rapid mixing of a 70 nM DNA polymerase and 120 nM ^{32}P-labeled primer/template containing DNA damage complex in reaction buffer (pH 7.4) with a second solution containing 1 mM dCTP and 5 mM Mg^{2+}, with or without 1.2 μM unlabeled trap primer/template without DNA damage in the same buffer. These two parallel reactions were performed for the same time and quenched with 0.6 M EDTA. The reaction products were quantified by denaturing gel electrophoresis, and the data points were fit with Eq. (6.2).

6.2.10 Phosphorothioate Analysis

In dNTP incorporation mechanism, the pre-steady-state kinetic analysis discovers the fast dNTP incorporation step, which includes the conformation change step and chemical bond formation step. These two steps cannot be distinguished by the pre-steady-state kinetic analytic method. In order to test which step is the rate-limiting step, phosphorothioate analysis was performed. Reactions were initiated by rapid mixing of ^{32}P-primer/template and polymerase mixtures with (S_p)-dNTPαS·Mg^{2+} complex (or dNTP·Mg^{2+}) and then quenched with 0.6 M EDTA after varying reaction times. Products were analyzed and quantified.

6.2.11 Stopped-Flow Fluorescence Measurements of Conformational Change

Auto SF-120 instrument (KinTek Corporation, USA) was used in the measurement of transient fluorescent assays. The 335-nm-long-pass filter (CVI Laser Corp., Albuquerque, NM) was used to eliminate the excitation light. A specific band-pass filter was used to only bypass the emission fluorescent signal.

Fluorescent probe was added to DNA or some specific location of protein. For Y-family Dpo4, Trp-239 can be a fluorescent probe to detect the conformational change, and for A-family T7 DNA polymerase, A fluorescent dye MDCC can be attached to the figure domain to probe conformational change.

Herein, we use Dpo4 T239W as an example to explain how to detect the conformation change using SF-120. $MgCl_2$ (5 mM) was included in both syringes. In typical experiments for measuring the effect of dNTP binding on fluorescence of the Dpo4 T239W, one syringe contained Dpo4 T239W and DNA in 50 mM Tris-HCl buffer (pH 7.5 at 25 °C) containing 50 mM NaCl, 5 mM dithiothreitol, and 5 % (v/v) glycerol, and the second syringe contained various concentrations of the correct dNTP in the same Tris buffer. After rapid mixing, the final concentration of Dpo4:DNA was 1 μM. In all cases, standard assays were performed including all components except the reagent producing a change (e.g., dNTP in the case of fluorescence changes versus dNTP concentrations). The fluorescence plots measured here represent the averages of eight different shots. The rates of conformation change at different dNTP concentrations can be obtained by nonlinear regression fitting the fluorescence increase signal against time using the equation:

$$y = A\left(1 - e^{-k_{obs}t}\right) \tag{6.5}$$

where y is the fluorescence signal produced over time, A is the amplitude of the signal, k_{obs} is the observed rate constant, and t is time. The k_{obs} apparent values were then plotted against dNTP concentrations using the hyperbolic equation (Eq. 6.6) to obtain the ground state dissociation constant of dNTP ($K_{d,dNTP}$), maximal forward conformation change rate (k_3), and reverse conformation change rate (k_{-3}):

$$k_{obs} = k_3[\text{dNTP}] / \left(K_{d,dNTP} + [\text{dNTP}]\right) + k_{-3} \tag{6.6}$$

All nonlinear regression analysis used GraphPad Prism Version 3.0.

6.2.12 Kinetic Simulations

In order to study each parameter at each step of dNTP incorporation mechanism, kinetic simulations were performed using a minimal mechanism using DynaFit (BioKin, Pullman, WA) (Fig. 1.1). Due to the presence of DNA damage, the minimal mechanism might not fit the experimental data. Some modified mechanisms with the presence of a nonproductive ternary complex were used to fit experimental data. The least squares fit to the experimentally determined data were calculated.

6.3 LC-MS/MS Sequence Analysis of Extension Products Beyond DNA Damage

6.3.1 Materials

The materials were as follows: DNA polymerase, damaged and undamaged ssDNAs, Tris-HCl buffer (pH 7.5), NaCl, dithiothreitol, dNTP, $MgCl_2$, *E. coli* uracil DNA glycosylase, piperidine, EDTA, $NH_4CH_3CO_2$, and CH_3CN.

6.3.2 Preparation Sample of DNA Extension Products Beyond DNA Damage

DNA polymerase (5 μM) was incubated with uracil-containing primer/template DNA (10 μM), all four dNTPs (1 mM each), and $MgCl_2$ (5 mM) in a final volume of 100 μl at 37 °C for 4 h in 50 mM Tris-HCl buffer (pH 7.4) containing 5 mM dithiothreitol. Reactions were terminated by extraction of the remaining dNTPs using a size-exclusion chromatography column (Bio-Spin 6 chromatography column, Bio-Rad). Concentrated stocks of Tris-HCl, dithiothreitol, and EDTA were added to adjust the concentrations to 50, 5, and 1 mM, respectively. Next, *E. coli* uracil DNA glycosylase (20 units, Sigma-Aldrich) was added, and the solution was incubated at 37 °C for 6 h to hydrolyze the uracil residues on the extended primer. The reaction mixture was then heated at 95 °C for 1 h in the presence of 0.25 M piperidine (to break the primer chain at the abasic sites), followed by removal of the solvent by centrifugation under vacuum. The dried sample was resuspended in 100 μl of H_2O for MS analysis.

6.3.3 LC-MS/MS Sequence Analysis of Extension Products

LC-MS/MS analysis was performed on a Waters Acquity UPLC system (Waters, Milford, MA) connected to a Finnigan LTQ mass spectrometer (Thermo Fisher Scientific, Waltham, MA), operating in the ESI negative ion mode. An Acquity UPLC BEH octadecylsilane (C_{18}) column (1.7 mm, 1.0 mm × 100 mm) was used with the following LC conditions: Buffer A contained 10 mM $NH_4CH_3CO_2$ plus 2 % CH_3CN (v/v) and buffer B contained 10 mM $NH_4CH_3CO_2$ plus 95 % CH_3CN (v/v). The following gradient program was used with a flow rate of 150 μl min^{-1}: 0–2.5 min, linear gradient from 100 % A to 95 % A/5 % B (v/v); 2.5–6.0 min, linear gradient to 75 % A/25 % B (v/v); 6–6.5 min, linear gradient to 100 % B; 6.5–8.0 min, hold at 100 % B; 8.0–9.0 min, linear gradient to 100 % A; 9.0–12.0 min, hold at 100 % A. The temperature of the column was maintained

at 50 °C. Samples were injected with an autosampler system. ESI conditions were as follow: source voltage 4 kV, source current 100 mA, auxiliary gas flow rate setting 20, sweep gas flow rate setting 5, sheath gas flow setting 34, capillary voltage −49 V, capillary temperature 350 °C, tube lens voltage −90 V. MS/MS conditions were as follows: normalized collision energy 35 %, activation Q 0.250, and activation time 30 ms. The doubly (negatively) charged species were generally used for CID analysis. The calculations of the CID fragmentations of oligonucleotide sequences were done using a program linked to the Mass Spectrometry Group (Medicinal Chemistry) at the University of Utah (www.medlib.med.utah.edu/massspec).

6.4 X-Ray Crystal Structure Analysis of DNA Polymerase with DNA Containing DNA Damage

6.4.1 Materials

The materials were as follows: DNA polymerase, damaged and undamaged ssDNAs, Tris-HCl buffer (pH 7.5), NaCl, glycerol, 2-mercaptoethanol, dNTP, $MgCl_2$, polyethylene glycol 3350, and ethylene glycol.

6.4.2 Crystallization of Polymerase with DNA Containing DNA Damage

Different polymerases have different crystallization methods. Here, we use Dpo4 and N2-NaphG as models to explain the crystallization process. A 18-mer template containing N2-NaphG and 14-mer primer containing a 3′-terminal dideoxycytidine were annealed to form a duplex. Dpo4 was mixed with DNA (1:1.2 molar ratio) in 20 mM Tris-HCl buffer (pH 8.0, 25 °C) containing 60 mM NaCl, 4 % glycerol (v/v), and 5 mM 2-mercaptoethanol and then placed on ice for 1 h prior to incubation with 5 mM $MgCl_2$ and 1 mM dGTP. The final Dpo4 concentration was 10 mg/ml. Crystals were grown using the sitting-drop/vapor diffusion method with the reservoir solution containing 20 mM Tris-HCl (pH 8.0 at 25 °C), 15 % polyethylene glycol 3350 (w/v), 60 mM NaCl, 5 mM $MgCl_2$, and 4 % glycerol (v/v). Droplets consisted of a 1:1 (v/v) mixture of the Dpo4-DNA-Mg^{2+}-dGTP complex and the reservoir solutions and were equilibrated against the reservoir solutions. Crystals were soaked in mother liquor containing an additional 25 % polyethylene glycol 3350 (w/v) and 15 % ethylene glycol (v/v) and then swiped through paratone-N (Hampton Research, Aliso Viejo, CA) and flash frozen in a stream of liquid nitrogen.

6.4.3 X-ray Diffraction Data Collection and Processing

Two Dpo4-N^2-NaphG complex crystals were resolved. X-ray diffraction data for the Dpo4-N^2-NaphG complex crystals (Npg-1 and Npg-2) were collected at the Advanced Photon Source (Argonne National Laboratory, Argonne, IL) on the 21-ID (LS-CAT) and 22-ID (SER-CAT) beam lines, respectively. Both data sets were recorded from cryoprotected crystals using a wavelength of 0.98 Å at 110 K. The crystals diffracted to 3.0-Å resolution. Individual frames were indexed and scaled with the program XDS (Npg-1) or HKL2000 (60) (Npg-2). Both complex crystals belong to space group P21212. X-ray diffraction data collection and processing statistics should be listed.

6.4.4 Structure Determination and Refinement

The structure of Dpo4 containing N^2-NaphG should be refined based on a known and similar structure. A wild-type Dpo4-G complex (pdb accession code 2bqr) minus solvent molecules, template residue 5, metal ions, and dGTP was used as the starting model for Npg-1. Molecular replacement was performed using MOLREP as a part of the CCP4 program suite. The refined structure of the Npg-1 complex (minus solvent molecules, template residue 5, metal ions, and dGTP) served as the starting model for the Npg-2 structure, and the locations of the individual models were optimized by several rounds of rigid body refinement while gradually increasing the resolution of the diffraction data. Manual model rebuilding was done with the program TURBO-FRODO. The maps were computed using the sA-modified coefficients. Clear positive density for the Mg^{2+} ions and the dGTP was observed in the initial difference Fourier electron density maps of both complexes, although the positive density was sparser for dGTP in the Npg-1 structure. Positive density was observed for the N^2-NaphG-modified template residue, but several rounds of modeling and refinement were required to ascertain the final orientation of the base and the naphthalene moiety in both structures. The CNS package was used for the refinement of the models by performing simulated annealing, gradient minimization, and refinement of individual isotropic temperature and occupancy factors. The statistics of the refined models for all structures should be summarized. The crystallographic figures were prepared using PyMOL. Calculation of the DNA helical parameter descriptions was performed using CURVES.

Further Reading

Goodman MF, Creighton S, Bloom LB, Petruska J (1993) Biochemical basis of DNA replication fidelity. Crit Rev Biochem Mol Biol 28:83–126

Zang H, Irminia A, Choi JY, Angel KC, Loukachevitch LV, Egli M, Guengerich FP (2006) Efficient and high fidelity incorporation of dCTP opposite 7,8-dihydro-8-oxo-deoxyguanosine by Sulfolobus solfataricus DNA polymerase Dpo4. J Biol Chem 281:2358–2372

Johnson KA (1995) Rapid quench kinetic analysis of polymerases, adenosinetriphosphatases, and enzyme intermediates. Method Enzymol 249:38–6

Choi YJ, Guengerich FP (2004) Analysis of the effect of bulk at N2-alkylguanine DNA adducts on catalytic efficiency and fidelity of the processive DNA polymerase T7 exonuclease$^-$ and HIV-1 reverse transcriptase. J Biol Chem 279:19217–19229

Zang H, Goodenough AK, Choi JY, Irminia A, Loukachevitch LV, Kozekov ID, Angel KC, Rizzo CJ, Egli M, Guengerich FP (2005) DNA adduct bypass polymerization by Sulfolobus solfataricus DNA polymerase Dpo4. Analysis and crystal structures of multiple base-pair substitution and frameshift product with the adduct 1,N2-ethenoguanine. J Biol Chem 280:29750–29764

Zang H, Harris TM, Guengerich FP (2005) Kinetics of nucleotide incorporation opposite DNA guanine-N2 adducts by the processive bacteriophage T7- polymerase DNA. J Biol Chem 280:1165–1178

Patel SS, Wong I, Johnson KA (1991) Pre-steady-state kinetic analysis of processive DNA replication including complete characterization of an exonuclease-deficient mutant. Biochemistry 30:511–525

Furge LL, Guengerich FP (1997) Analysis of nucleotide insertion and extension at 8-oxo-7,8-dihydroguanine by replicative T7 polymerase exo- and human immunodeficiency virus-1 reverse transcriptase using steady-state and pre-steady-state kinetics. Biochemistry 36:6475–6487

Zang H, Goodenough AK, Choi JY, Irminia A, Loukachevitch LV, Kozekov ID, Angel KC, Rizzo CJ, Egli M, and Guengerich FP (2005) DNA adduct bypass polymerization by Sulfolobus solfataricus DNA polymerase Dpo4 - Analysis and crystal structures of multiple base pair substitution and frameshift products with the adduct 1,N-2-ethenoguanine. J Biol Chem 280:29750–29764

Vagin A, Teplyakov A (1997) MOLREP: an Automated Program for Molecular Replacement. J Appl Crystallogr 30:1022–1025

Vellieux FMD, Dijkstra BW (1997) Computation of Bhat's OMIT maps with different coefficients. J Appl Crystallogr 30:396–399

Brunger AT, Adams PD, Clore GM, DeLano WL, Gros P, Grosse-Kunstleve RW, Jiang JS, Kuszewski J, Nilges M, Pannu NS, Read RJ, Rice LM, Simonson T, Warren GL (1998) Crystallography & NMR system: A new software suite for macromolecular structure determination. Acta Crystallogr Sect D Biol Crystallogr 54:905–921

Lavery R, Sklenar H (1989) Defining the structure of irregular nucleic acids: conventions and principles. J Biomol Struct Dynam 6:655–667

Beckman JW, Wang Q, Guengerich FP (2008) Kinetic Analysis of Correct Nucleotide Insertion by a Y-family DNA Polymerase Reveals Conformational Changes Both Prior to and following Phosphodiester Bond Formation as Detected by Tryptophan Fluorescence. J Biol Chem 283:36711–36723

Zhang H, Lee S, Richardson, Charles C (2012) The roles of tryptophans in primer synthesis by the DNA primase of bacteriophage T7. J Biol Chem 287:23644–23656

Zhang H, Eoff RL, Kozekov ID, Rizzo CJ, Egli M, Guengerich FP (2009) Versatility of Y-family Sulfolobus solfataricus DNA Polymerase Dpo4 in Translesion Synthesis Past Bulky N-2-Alkylguanine Adducts. J Biol Chem 284:3563–3576

Zhang H, Beckman JW, Guengerich FP (2009) Frameshift Deletion by Sulfolobus solfataricus P2 DNA Polymerase Dpo4 T239 W Is Selective for Purines and Involves Normal Conformational Change Followed by Slow Phosphodiester Bond Formation. J Biol Chem 284:35144–35153

Zhang H, Eoff RL, Kozekov ID, Rizzo CJ, Egli M, Guengerich FP (2009) Structure-Function Relationships in Miscoding by Sulfolobus solfataricus DNA Polymerase Dpo4 Guanine N-2,N-2-dimethyl substitution produces inactive and miscoding polymerase complexes. J Biol Chem 284:17687–17699